DTIC FILE COPY,

May 1990   Thesis/Dissertation

Precipitation Rate Computations in the Tropics By The
Global Heat Budget Technique From 1 June 1984-31 May 1987

Keith Herman North

AFIT Student at: Purdue University

AFIT/CI/CIA - 90-085

AFIT/CI
Wright-Patterson AFB OH 45433

DTIC
ELECTE
OCT 24 1990
S
E
D

77

PURDUE UNIVERSITY
GRADUATE SCHOOL
Thesis Acceptance

This is to certify that the thesis prepared

By ____Keith H. North_____

Entitled

Precipitation Rate Computations in the Tropics by the
Global Heat Budget Technique From 1 June 1984 - 31 May 1987.

Complies with University regulations and meets the standards of the Graduate School for originality and quality

For the degree of __Master of Science_____

Signed by the final examining committee:

_____Dayton D. Vincent_____ , chair

_____Phillip J. Smith_____

_____Krishnamurthy_____

_____

Approved by:

_____[signature]_____   20 Apr. 1990
Department Head   Date

☐ is
This thesis ☒ is not to be regarded as confidential

_____Dayton D. Vincent_____
Major Professor

PRECIPITATION RATE COMPUTATIONS IN THE TROPICS

BY THE GLOBAL HEAT BUDGET TECHNIQUE

FROM 1 JUNE 1984 - 31 MAY 1987

A Thesis

Submitted to the Faculty

of

Purdue University

by

Keith Herman North

In Partial Fulfillment of the

Requirements for the Degree

of

Master of Science

May 1990

ACKNOWLEDGEMENTS

I would like to thank Dr. Vincent for his patient help over the past two years. I especialy appreciate his willingness to answer the same question more than one time. Thanks also to Dr. Smith and Dr. Harshvardhan for their constructive comments throughout my research.

My two office-mates, and good friends, were very helpful. Perry and Jim's math lessons were an 'integral' part of my success.

My best friend (and wife), Susie, deserves at least half the credit for this thesis. Throughout our ten years of marriage she constantly encouraged me to go to school and would not let me quit (even when I acted weird!). Thanks also to Evangeline and William (our children) for all the artwork they supplied to keep my office cheerful.

Finally, and most importantly, I want to thank Jesus Christ. Even when I have failed you, you have been faithful to me. Thank you. As the angels in heaven proclaim "You alone are worthy!"

TABLE OF CONTENTS

LIST OF TABLES

LIST OF FIGURES

ABSTRACT

North, Keith Herman, M.S., Purdue University, May 1990. Precipitation Rate Computations in the Tropics by the Global Heat Budget Technique from 1 June 1984 - 31 May 1987. Major Professor: Dr. Dayton G. Vincent.

This study presents monthly maps of computed precipitation rates over the tropics (30°N to 30°S) which were derived from the "apparent" heat source (Q_1) budget method. The data set used was the WMO archive version of the ECMWF global analysis data set for the period, 1 June 1984 - 31 May 1987.

The Q_1-budget technique computes the total derivative of grid-scale dry static energy at increments of 2.5° longitude by 2.5° latitude at seven pressure levels (1000, 850, 700, 500, 300, 200 and 100 mb). When vertically integrated this quantity is equivalent to the total diabatic heating. Values of some of the diabatic heating terms are estimated and used in conjunction with mean monthly OLR values, generated from NOAA daily polar orbiter data, to solve for precipitation as the residual in the budget equation.

Annual precipitation rate maps are presented and compared with annual average maps from atlases by Jaeger and by Dorman and Bourke, as well as limited island station data. The results compare favorably with both atlases and show an average error of 15% when compared to a ten year annual average of observed island and coastal station data. The computed precipitation rates were latitudinally averaged and compared to Dorman and Bourke's results for January, July, and annual means. In addition, time series of monthly-averaged precipitation rates are shown and discussed

with regard to spatial and temporal variations, for selected regions, with particular attention devoted to the Southern Hemisphere.

1. INTRODUCTION

The tropics produce an enormous surplus of energy which is essential to maintain the observed global scale circulation patterns. One of the goals of this study is to gain a greater understanding of the heating potential the tropics possess by examining the "apparent" heat source (Q_1), i.e., dry static energy budget (e.g., Yanai et al., 1973), for the period, June 1984-May 1987. Another goal is to convert Q_1 into a precipitation rate, which is possible if both the net radiation in an atmospheric column and sensible heat exchange with the underlying surface are known. In the remainder of this chapter the impetus for this study is discussed. In Chapter 2 the data sources and computational methods are reviewed. This is followed by a discussion of results in Chapter 3 and a brief summary and some recommendations in Chapter 4.

1.1 Importance of Tropical Heating

Since the tropics cover one-half of the earth's surface, a better understanding of the physical and dynamical processes at work there is essential to a better understanding of global circulation patterns. Lau and Chan (1983) showed that significant teleconnections exist between the Central Pacific and extratropical regions. Within the tropics latent heat release appears to be the primary energy source (Holton, 1979). In the tropics moisture-laden air converges and rises causing condensation, and a significant amount of heat is released in towering cumulonimbus clouds that extend through the entire troposphere (Riehl and Simpson, 1979). The resulting convective zones are characterized by heavy precipitation and low surface pressures. In the upper troposphere air diverges and, drained of moisture, subsides over regions with minimal

rainfall and high surface pressures. While subsiding, the air radiates heat to space. Thus, the tropical atmosphere can be viewed as a heat engine where latent heat is gained from convection and heat is lost by radiation to space (Emmanuel, 1988).

Most of the latent heat release occurs in convective cloud systems that are embedded in larger scale circulations; therefore, its effect cannot be measured directly, and estimates of this important quantity must be made. The traditional way of estimating latent heat release is through the use of a cumulus parameterization scheme. Cumulus parameterization schemes use large-scale data to model an ensemble of cooperative cloud elements since available data do not allow computation of latent heat from individual clouds. Because the convective processes are subgrid scale, all schemes require assumptions. Frank (1983) provides an excellent review of the cumulus parameterization problem.

Parameterization models can be divided into two groups:

    1) Mesoscale parameterization models, and

    2) Coarse grid scale models.

Mesoscale models are used with fine grid meshes (<50 km) and are not a concern here. Coarse grid models, however, need to parameterize the mutual interactions of convective and mesoscale processes. Traditionally, there have been three coarse grid model schemes used to parameterize latent heat: 1) moist convective adjustment (Manabe et al., 1965); 2) moisture convergence with cloud models, commonly known as the Kuo (1965, 1974) scheme; and 3) the Arakawa and Schubert (1974) scheme. The moist convective adjustment scheme bypasses most of the physical processes involved through the use of variable lapse rates, and has limited flexibility. The Kuo scheme's biggest problem is the need to specify moisture and heat partitioning vertically throughout the cloud model and this is a poorly understood process. The Arakawa and Schubert scheme, like all the other coarse grid schemes, has problems related to the

resolution of mesoscale circulations and their interactions with convective processes. Frank concludes his review of the cumulus parameterization problem by writing, "with almost every new observational or theoretical discovery there is a new constraint upon parameterization. It seems ever less likely that a comprehensive scheme or even approach will emerge to satisfy all models."

An alternative scheme to parameterization is the budget technique. An example of this technique is the aforementioned "apparent" heat source (Q_1) budget, which is used in the present study. More will be said later concerning this technique.

1.2 Present Status of Global Precipitation Estimates

Since the primary impetus for using the heat budget method is to obtain precipitation rates, it is appropriate to look at the methods presently used to obtain these estimates, as well as the current status of what is known about global precipitation. The earliest attempts (about 400 B.C.) at measuring surface precipitation were in India using bowls about 46 cm in diameter. Apparently, the information was used to help determine the annual crop that was to be sown. It was not until 1722 that Rev. Horsley related the diameter of the catch to the diameter of the container, and scaled the container accordingly, to produce a rain gage similar to our present one (Middleton, 1969).

In the early 1940's, radar was first used to track rain storms. By the late 40's a theoretical relation between backscatter energy and rainfall rate was developed. Battan (1973) has an extensive discussion on various methods used to estimate rainfall rates and total rainfall through the use of radar.

The newest method of estimating precipitation is through the use of satellite data. Early efforts focused on estimating the probability of precipitation as a function of the 'window temperature'. In the mid 70's the microwave technique related

electronically scanning microwave radiometer (ESMR) brightness temperatures to hourly rain rates. By 1980, useful qualitative results (i.e. probability of rain) were obtained but the quantitative picture was still rather uncertain (Flueck, 1981).

Other satellite techniques have been developed to estimate rainfall using visible and/or infra-red (IR) imagery. In general these methods correlate rainfall with bright (visible) cold (IR) clouds. Arkin and Meisner (1987) review the IR approach to estimation of precipitation using fractional cloud coverage. At this time IR methods produce better results than microwave methods and are most accurate over oceanic areas.

Mintz (1981) presented a review of the present status of global precipitation estimates. Jaeger (1976) produced the only estimate we have of normal monthly precipitation over the entire globe. Over the oceans Jaeger simply took the annual precipitation as given by Geiger (1965), and distributed that precipitation over the twelve months of the year. Geiger's distribution in turn can be traced back to Schott (1926). For the Atlantic Ocean, Schott reworked the earlier analysis of Supan (1898) which was computed from the logs of ships crossing the oceans. Dorman and Bourke (1979, 1981) give the annual distributions of precipitation over the Atlantic and Pacific Oceans using Tucker's (1961) method and a latitude-derived correction for the air temperature (Dorman and Bourke, 1978). The estimates of Jaeger (1976), Dorman and Bourke (1978, 1979, 1981), and Dorman (1981) will be compared to the heat budget results obtained in this study. Unfortunately, Dorman and Bourke's results for the Atlantic are only available for seasonal averages (Dorman, personal communication).

1.3 Objectives of Present Study

The work presented here is an expansion of the research conducted by Pedigo and Vincent (1990), hereafter referred to as PV. They examined the Q_1 budget and precipitation rates for a portion of the first Special Observing Period (SOP-1) of The Global Weather Experiment (FGGE) using the Level III-b analyses produced by the NASA Goddard Laboratory for Atmospheres (GLA). The present study examines the Q_1 budget and precipitation rates over a three year period using a routine data set: the European Center for Medium-range Weather Forecasts (ECMWF) twice daily grid point analyses. In addition, PV used the GLA general circulation model (GCM) values of net radiation and sensible heat. These values were not available for the present study and had to be estimated. More will be said in the next chapter about assumptions, data and computational procedures. The specific objectives of the thesis are to:

1) compute Q_1 budget terms for the global tropics from 1 June 1984 to 31 May 1987;

2) calculate precipitation rates as the residual in the Q_1 budget;

3) examine the spatial variability of tropical rainfall rates among several geographical regions, with a focus on those in the Southern Hemisphere;

4) examine the temporal variability of rainfall rates on a monthly basis over the three year period; and

5) compare the present precipitation rates to those obtained by previous investigators.

2. DATA AND COMPUTATIONAL PROCEDURES

The data set used in this study was the WMO archive version of the ECMWF global analysis data set. The data set includes upper air grid point fields for six physical parameters (geopotential height, temperature, horizontal wind components, vertical velocity and relative humidity) at seven pressure levels (1000, 850, 700, 500, 300, 200, and 100 mb), except for relative humidity which was analyzed only up to 300 mb. Each parameter on each pressure level is stored as a field of grid point values on a 2.5° x 2.5° regular rectangular mesh. Trenberth and Olson (1988b) give a full description of the data set. They compared the analyses from the ECMWF to those from the National Meteorological Center (NMC), with the conclusion that the ECMWF analyses are superior in some respects (Trenberth and Olson, 1988c). They further noted that a major model change to the ECMWF analyses on 1 May 1985 increased the divergent wind field in the tropics and cautioned that this might have an impact on heating and moisture distributions. Thus, in this study greater emphasis is placed on the results from June 1985 - May 1987.

2.1 The Q_1-Budget Equation

The development of the heat budget in this study follows the treatment of Yanai et al. (1973) and Thompson et al. (1979), and is identical to that presented by Miller and Vincent (1987) and PV. The budget equation is based on the First Law of Thermodynamics which can be written in the following form:

$$\frac{dh}{dt} = c_p \frac{dT}{dt} - \alpha \frac{dp}{dt},$$ (1)

where $\frac{dp}{dt} = \frac{\partial p}{\partial t} + V \cdot \nabla p + w \frac{\partial p}{\partial z}.$

It is frequently assumed that (Holton, 1979)

$\frac{\partial p}{\partial t} + V \cdot \nabla p$ is negligible compared to $w \, \partial p / \partial z$; therefore,

$\frac{dp}{dt} \approx w \frac{\partial p}{\partial z} = - \rho g \frac{dz}{dt}$ when hydrostatic balance is assumed.

Substitution into (1) yields:

$$\frac{dh}{dt} = c_p \frac{dT}{dt} + g \frac{dz}{dt} \quad \text{or}$$

$$\frac{dh}{dt} = \frac{d}{dt}(c_p T + \Phi).$$ (2)

From (2) we now define $s = c_p T + \Phi$, (3)

the dry static energy, which is the sum of enthalpy, ($c_p T$), and gravitational potential energy (Φ). Since dh/dt denotes total diabatic heating, we can write:

$$\frac{ds}{dt} = \frac{dh}{dt} = S_H,$$ (4)

where S_H = sources and sinks of heat.

Expanding the left side of (4) gives the heat budget per unit mass of air at any pressure level:

$$\frac{\partial s}{\partial t} + V \cdot \nabla s + \omega \frac{\partial s}{\partial p} = S_H.$$ (5)

Now, following the development given by PV, the variables in (5) can be partitioned into a spatially averaged component (overbar) and a departure from the spatial average (prime). Substitution according to this partitioning and use of the Equation of Continuity leads to the following:

$$Q_1 = \frac{\partial \bar{s}}{\partial t} + \bar{V} \cdot \nabla \bar{s} + \bar{\omega} \frac{\partial \bar{s}}{\partial p} = Q_R + Q_L - \nabla \cdot \overline{V's'} - \frac{\partial}{\partial p}(\overline{\omega's'}),$$ (6)

where Q_1 is the "apparent" heat source consisting of net radiation, Q_R, net condensational heating, Q_L, and the horizontal and vertical eddy flux convergences of dry static energy.

In the present study, grid point values of s, V, and ω are assumed to represent the spatial averages of the respective quantities over a 2.5° latitude by 2.5° longitude box surrounding the grid point. Thus, the contribution by the eddy terms in (6) could not be calculated. The horizontal eddy flux convergence, $-\nabla \cdot \overline{V's'}$, is conventionally assumed to be negligibly small compared to other terms (McBride, 1981) and therefore it is neglected hereafter. However, there appears to be no guarantee that $\partial/\partial p(\overline{\omega's'})$ is negligible (McBride, 1981). Thus, Q_1 must be interpreted as the diabatic heating plus the vertical eddy flux convergence of s. This is consistent with Yanai et al. where Q_1 is not described as a heat source but rather an "apparent" heat source. Consequently, the term Q_1-Q_R on an isobaric surface is physically interpreted as the total convective heating ($Q_L - \partial/\partial p(\omega's')$).

If (6) is vertically-integrated from 100 mb (p_t) to 1000 mb (p_b), the result is:

$$g^{-1} \int_{P_t}^{P_b} Q_1 \, dp = g^{-1} \int_{P_t}^{P_b} \frac{\partial \bar{s}}{\partial t} + \overline{V} \cdot \nabla \bar{s} + \bar{\omega} \frac{\partial \bar{s}}{\partial p} \, dp$$

$$= g^{-1} \int_{P_t}^{P_b} Q_R \, dp + P_0 + S_0 , \tag{7}$$

where P_0 is the net columnar condensational heating, assumed to be equal to the precipitation rate, and S_0 is the sensible heat exchange between the atmosphere and the underlying surface. The latter is assumed to be the only important contribution

from the vertical eddy flux term. Symbolically, (7) may be expressed as:

$$DSDT + HADS + VADS = Q_R + P_0 + S_0, \qquad (8)$$

where all terms are vertically-integrated and

DSDT = local rate of change of dry static energy or the storage of s,

HADS = horizontal advection of s, and

VADS = vertical advection of s.

The terms on the left side of (8) were computed from the ECMWF analyses at each pressure level. Horizontal space derivatives were computed from second-order, centered finite-difference approximations. The time derivative was calculated for a 12-h period using a centered time difference (00 GMT and 12 GMT). Two of the three diabatic heating terms on the right side of (8), Q_R and S_0, were estimated by methods described below, leaving P_0 as the unknown residual.

As will be seen, the major terms in the Q_1 budget are VADS, Q_R, and P_0. The fact that vertical advection of dry static energy is approximately balanced by the total diabatic heating in the tropics has long been known through scale analysis (Holton, 1979) and observational studies (Newell et al., 1974; McBride, 1981).

2.1.1 Sensible Heat

As noted earlier, values of S_0 were not available for the present study. In similar studies, Miller and Vincent (1987) and PV found that S_0 usually did not play a significant role in the Q_1 budget. This tendency was also found by Garstang (1967) and Rao et al. (1980) over the tropical oceans. Betts and Ridgway (1987) found S_0 to have a value of 10 Wm^{-2}. PV found S_0 to have a nearly constant value of 20 Wm^{-2} over water. This agrees well with Yanai who calculated a Bowen ratio of 0.076. Using Yanai's Bowen ratio for the same area in this study, yields $S_0 = 19$ Wm^{-2}. Thus, in the present study, S_0 was assumed to be 20 Wm^{-2} over the entire domain. This should

provide acceptable results, particularly over the oceans, which are the primary areas of interest.

2.1.2 Radiation Terms

Peng et al., (1982) calculated that, on a global basis, more than 50% of incoming solar radiation is absorbed at the surface. Two-thirds of this is absorbed in the tropical oceans between $\pm$ 30° latitude. A large portion of this energy is later transferred to the atmosphere in the form of latent heat. Chou (1985) discusses the cyclical nature of this process by noting that atmospheric and oceanic circulations are ultimately driven by solar radiation, then modulated by orography and the rotation of the earth. However, both the shortwave radiation absorbed and the longwave radiation emitted by the earth and its atmosphere are affected by the general circulation of the atmosphere and oceans. Obviously then, radiation plays an important role in determining the state of the atmosphere and must be carefully considered in the present analysis.

PV used model generated values of Q_R. However, similar data were not available as part of the ECMWF analyses used here. Therefore, the following scheme was incorporated, with the full knowledge that better estimates of radiational processes (see, for example, Gupta, 1989) would no doubt improve the rainfall rates obtained herein.

$$Q_R = OLR + S_a + N_s$$

where

OLR is the outgoing longwave radiation to space,

S_a is the atmospheric absorption of shortwave radiation, and

N_s is the net longwave radiation from the surface.

Conceptually the atmosphere can be thought of as a heat reservoir with OLR a measurement of the heat escaping out the top. Mean monthly OLR values were used as

a measure of the radiational cooling occurring at the top of the atmosphere. The monthly values were generated from National Oceanic and Atmospheric Administration (NOAA) daily polar orbiter data. The data were bilinearly interpolated to a 2.5° x 2.5° grid for direct use with the ECMWF grid. These data are routinely available from the National Climatic Data Center (NCDC). The values used were kindly supplied by Dr. W. Lau of GFSC/NASA and are the same as those given by Gruber et al. (1986).

Absorption of shortwave radiation (S_a) is fairly constant whether it is clear or cloudy. When it is clear, the low level water vapor in the atmosphere absorbs the shortwave radiation. When it is cloudy the clouds absorb the shortwave radiation, but, due to albedo changes, they also reflect off part of the incoming radiation. Thus, less shortwave radiation is available to be absorbed by the low level water vapor. The net result is the same as if there were clear skies. The global average of S_a is given by Wallace and Hobbs (1977) as 70 Wm^{-2}. For the tropics this value is closer to 80 Wm^{-2} (Harshvardhan, personal communication). However, for this study, ozone absorption of solar radiation above 100 mb (approximately 10 Wm^{-2}) needs to be subtracted from the tropical value; thus, S_a was set at a constant value of 70 Wm^{-2}.

Net longwave radiation from the surface (N_s) is one of the most difficult terms to estimate, since it is the most sensitive to cloud conditions. However, the high precipitable water content in the tropics dampens this variation to a great extent. Analysis of net surface values generated by Gupta (1989, and personal communication) show that the mean monthly value of net surface radiation over the tropical oceans is 50 Wm^{-2}. Chou (1985) and Wu and Cheng (1989) found that the net surface radiation is rather uniform with longitude and that the magnitude of the zonal variation of monthly net surface radiation is $\pm$20 Wm^{-2} about the mean of 50 Wm^{-2} in the tropical Pacific. Therefore, in the present study, a constant value of 50 Wm^{-2} is used for N_s, with an understanding that errors of approximately $\pm$20 Wm^{-2} can occur. This will yield errors

of $\pm$0.7 mm d^{-1} or approximately a 7% error in the convectively active regions (where typical rain rates are on the order of 10 mm d^{-1}). This assumption will lead to an overestimate (underestimate) of net surface radiation in areas where precipitation is occurring (not occurring) and, thus, a corresponding underestimate (overestimate) of the actual rainfall rate. In a precipitating area for example, the actual net surface radiation might be 40 Wm^{-2} rather than 50 Wm^{-2}. In this case the actual precipitation would be underestimated by 0.35 mm d^{-1}, which is not considered significant.

2.2 Advantages and Disadvantages of Budget Studies

A decided advantage of the heat budget method is that it is based on a fundamental conservation principle: the First Law of Thermodynamics. Another advantage lies in the fact that the heat budget terms are readily available and the scheme is computationally simple compared to the parameterization schemes. Also, this method is very inexpensive to apply compared to the cost of setting up a rain gauge network, radar sites or a satellite system.

A disadvantage of the budget method is that it fails to capture subgrid scale activity (as do the cumulus parameterization schemes). This problem is greatly diminished in this study since its focus is on annual and monthly-averaged values. In the form presented here, there is no prognostic capability; however, as model-generated values of vertical motion increase in accuracy this method might be used to forecast precipitation.

It is worth noting that, because of the assumptions made (e.g., neglecting $V \cdot \nabla p$ in (1) and assuming constant values of S_o and N_s), the most reliable estimates of precipitation occur over the tropical oceans. In one sense, this can be considered an advantage since this is the region where conventional estimates are lacking.

3. RESULTS AND DISCUSSION

This chapter begins by looking at the contribution of individual Q_1 terms in section 3.1. Section 3.2 displays Hovmoeller diagrams of Q_1 over the three year period of study. Section 3.3 presents the results of a sensitivity study for January 1986. Section 3.4 contains a discussion of the annual precipitation patterns compared with the results obtained by various other authors. Section 3.5 discusses monthly precipitation patterns. Finally, section 3.6 contains a review of the regional precipitation patterns found over the period of study.

3.1 Contributions of Q_1-Budget Terms

Figures 1, 2, and 3 show the contributions by DSDT, HADS, and VADS to Q_1, in the tropics, for January and July 1986. Although this information was computed for all 36 months, January and July were selected as being representative of the extremes. Figure 4 shows the "apparent" heat source, Q_1, which is the algebraic sum of Figs. 1-3, for January and July 1986. DSDT has a range of values between ± 10 Wm^{-2} over the oceanic areas and is found to be an order of magnitude less than the sum of HADS and VADS. Therefore, further commentary on DSDT is not offered.

The maps of HADS show a noteworthy, though not totally unexpected, feature. There are sharp gradients in HADS observed in the subtropical regions of the Northern and Southern Hemispheres during their respective winters. In mid-latitudes, ∇T and $\nabla \phi$ are larger than in the tropics and, thus, the advection of these terms ($V \cdot \nabla T$, $V \cdot \nabla \phi$) also increases. Between about 20N to 20S, HADS is observed to be fairly constant and relatively unimportant compared to VADS.
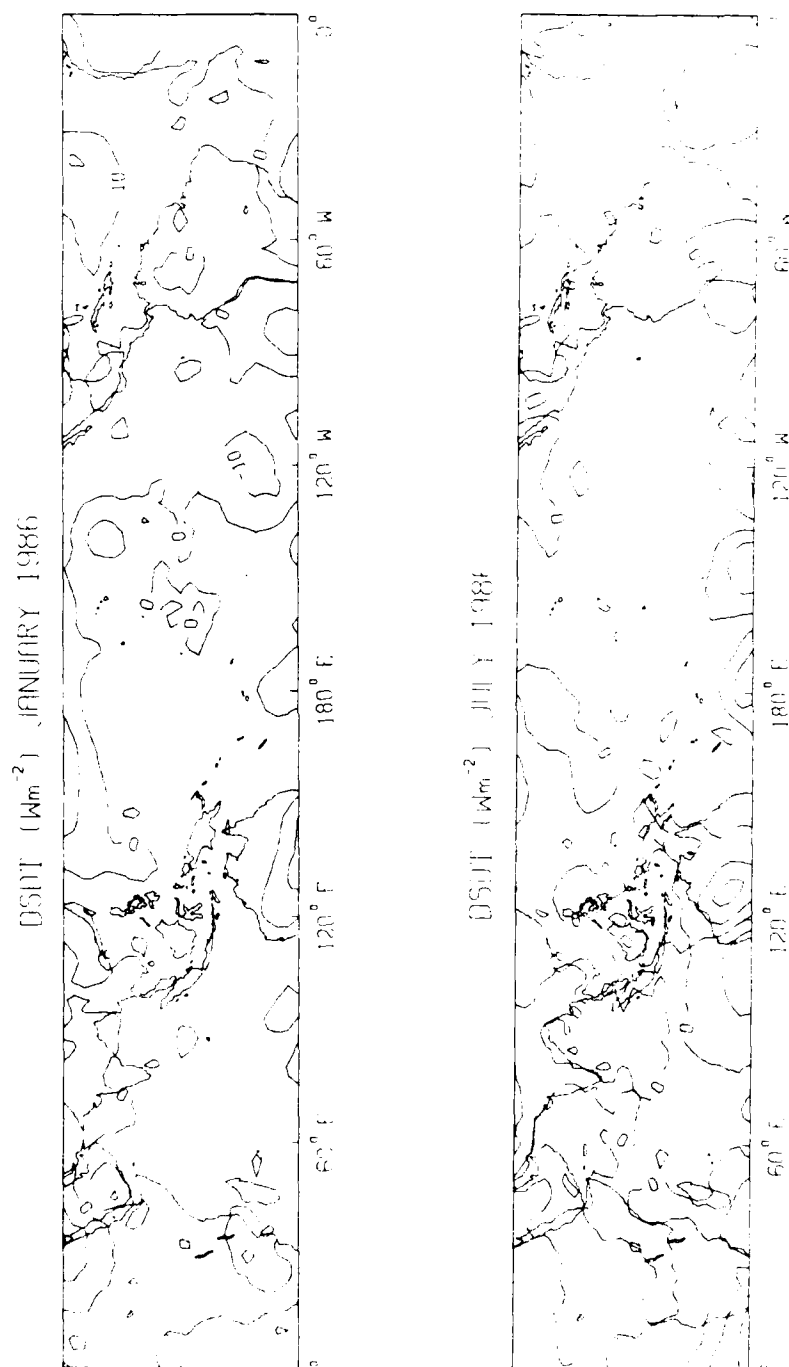
Figure 1. Time averaged contribution to the "apparent" heat source, Q_1, for January and July 1986 from DSDT (Contours are 10 Wm^{-2}).

Figure 2. Time averaged contribution to the "apparent" heat source, Q_1, for January and July 1986 from HADS (Contours are 100 Wm^{-2}) values $\geq$ 100 Wm^{-2} are shaded.

Figure 3. Time averaged contribution to the "apparent" heat source, Q_1, for January and July 1986 from VADS (Contours are 200 Wm^{-2}) values $\geq$ 200 Wm^{-2} are shaded.
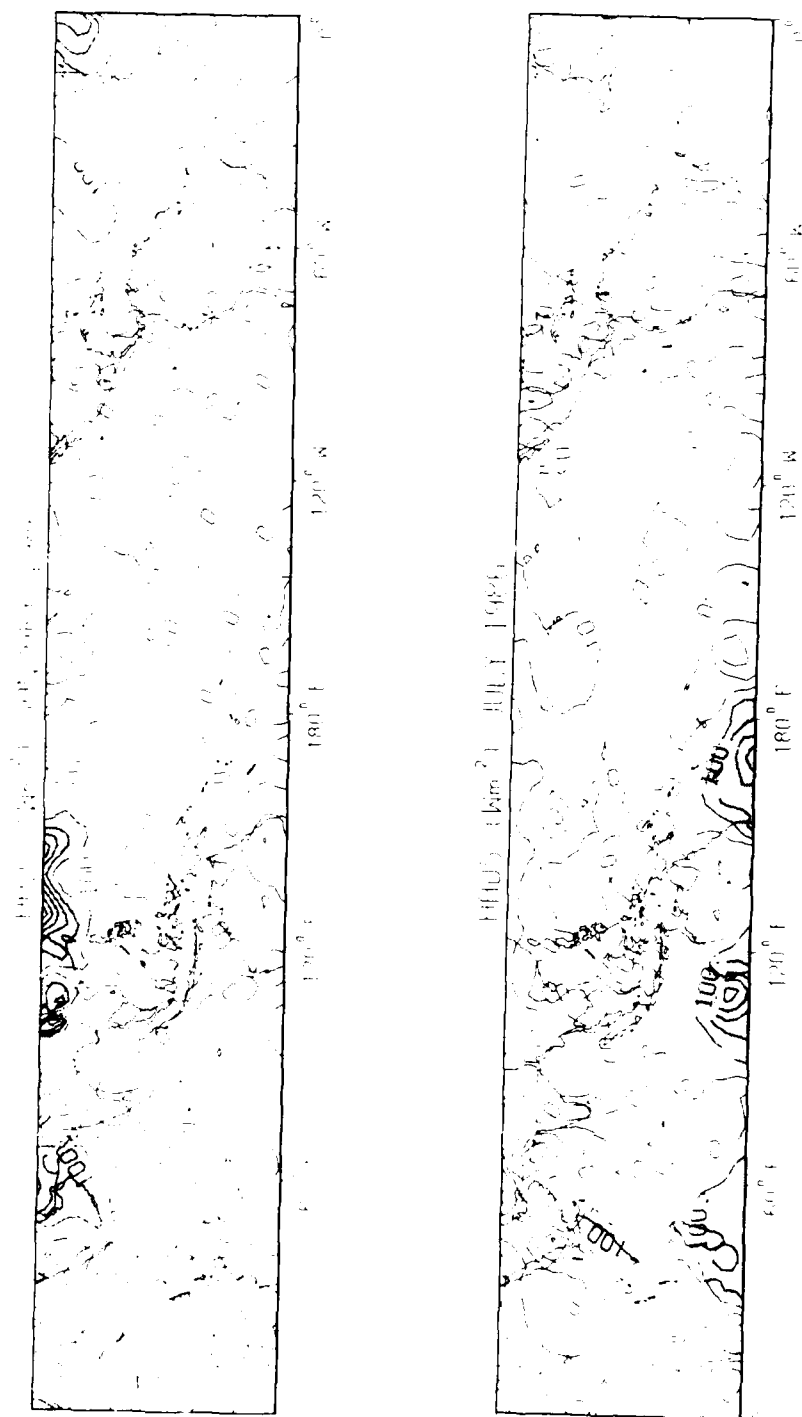
Figure 4. Time averaged maps of the "apparent" heat source, Q_1, for January and July 1986 (Contours are 200 Wm^{-2}) values $\geq$ 200 Wm^{-2} are shaded.
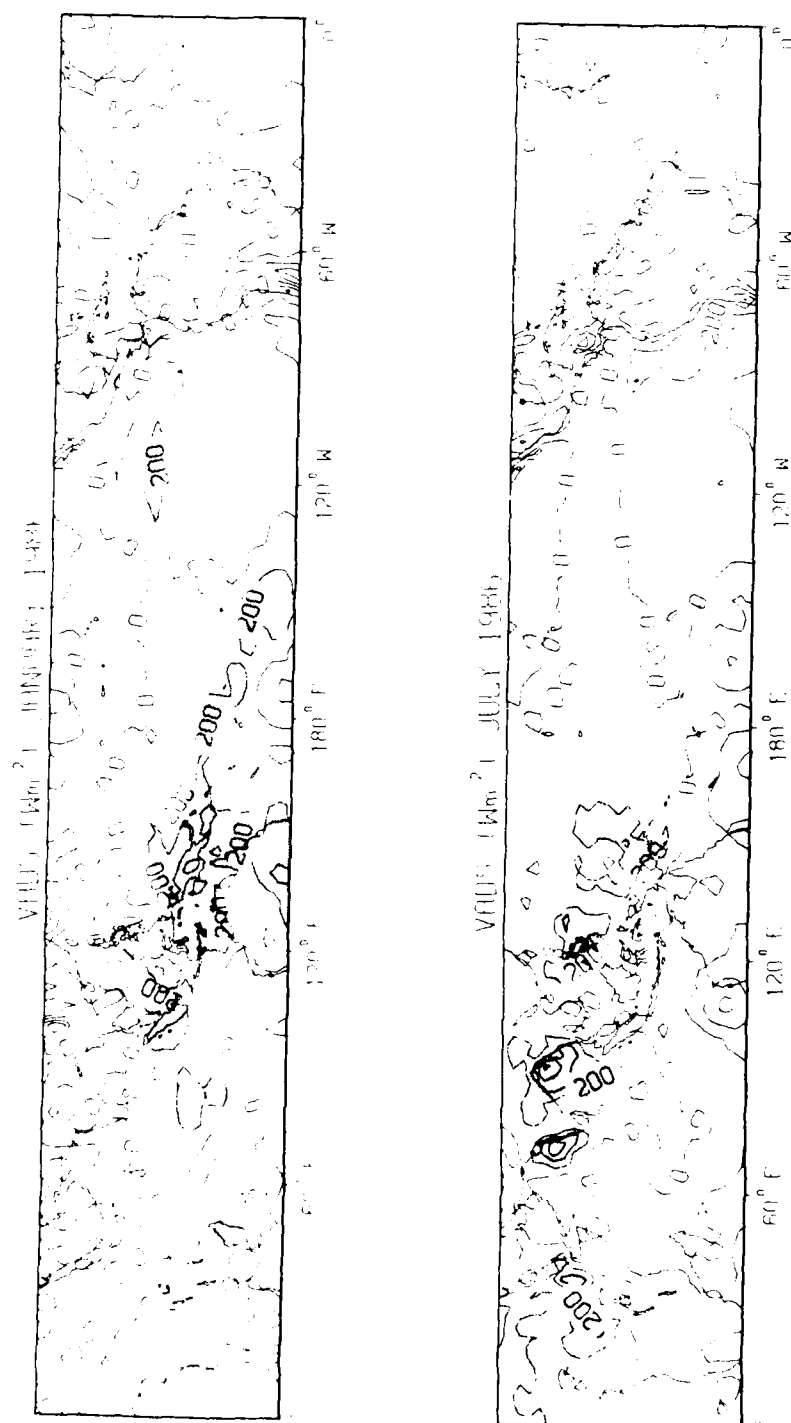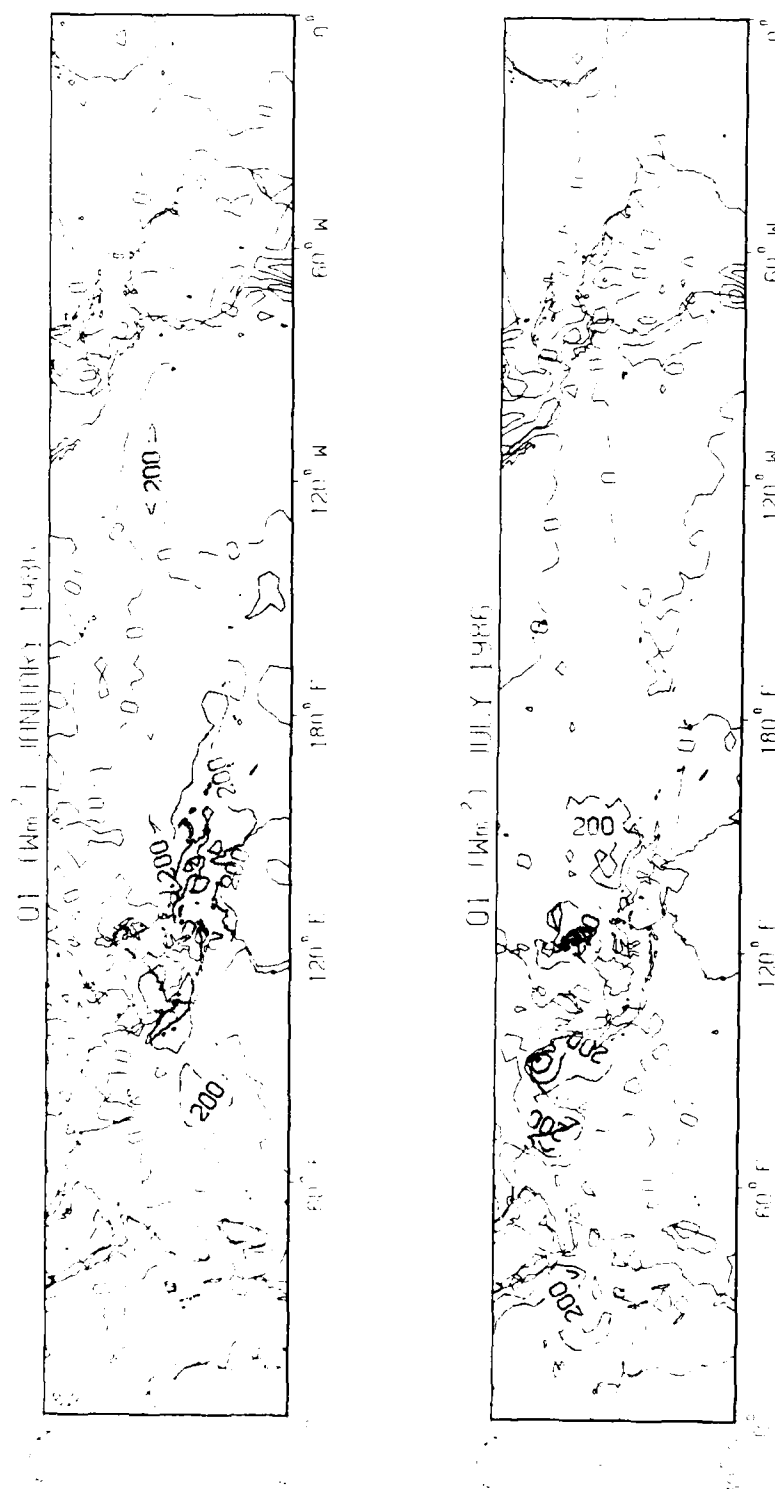
OLR (Wm^{-2})   JULY 1986

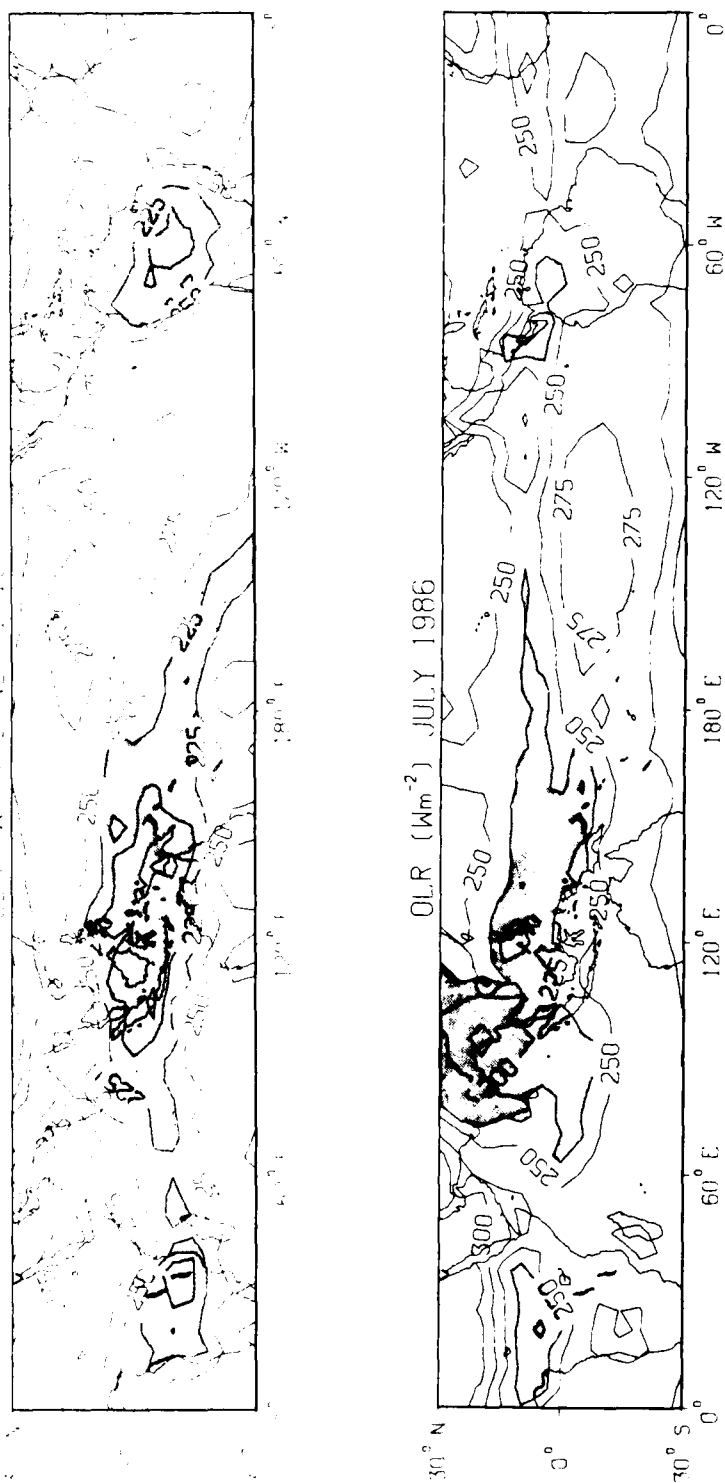Figure 5. Outgoing Longwave Radiation (OLR) maps for January and July 1986 in Wm^{-2} values $\leq$ 225 Wm^{-2} are shaded.

VADS is the dominant term over the majority of the tropics. Values ranging from approximately -200 to +200 Wm^{-2} are commonly seen. Note the large values of VADS associated with the ITCZ near Australia extending eastward to the SPCZ during January 1986. In July 1986 this maximum is shifted northward following the annual migration of the ITCZ. Also, note the large negative values of VADS off the west coast of South America, which indicates that diabatic cooling processes dominate in this region.

The map of Q_1, Fig. 4, most closely resembles that of VADS (Fig. 3), since over the majority of the domain VADS is dominant. Comparing the map of Q_1 to a map of OLR values (Fig. 5) shows an inverse relationship between the two, over oceanic regions. Low OLR values (≤ 225 Wm^{-2}) are associated with high (≥ 200 Wm^{-2}) Q_1 values. An example of this is seen in the SPCZ region during January 1986. Conversely, areas of high OLR values (≥ 275 Wm^{-2}) are associated with low Q_1 values. An example of this is seen off the west coast of South America where Q_1 values are negative. This relationship was expected since OLR values ≤ 225 Wm^{-2} are generally indicative of deep convection in the tropics (Heddinghaus and Krueger, 1981).

Table 1 presents regional averages of Q_1 budget terms in Wm^{-2} and precipitation rates in Wm^{-2} and in mm d^{-1} for January and July 1986. The regions, which are depicted in Fig. 6, were longitudinally defined as: South Africa (SAFR) 5E to 40E; Indian Ocean (IND O.) 50E to 100E; Australia (AUST) 110E to 165E; South Pacific Convergence Zone (SPCZ) 170W to 135W; South American Convergence Zone (SACZ) 70W to 25W. All the regions were latitudinally averaged from 0° to 30°S.

Table 1 shows that DSDT is generally positive in January in the Southern Hemisphere, indicating local increases in s, while it is negative or less positive throughout the Southern Hemisphere in July. In all cases, DSDT is negligible compared to other terms. Although HADS is larger than the DSDT term, in general, it

Table 1. Regional averages of Q_1 budget terms in Wm^{-2} and precipitation rates in Wm^{-2} and mm d^{-1} for January and July 1986.[1]

Region	Mo	DSDT	HADS	VADS	Q_1	Q_R	P_o Wm^{-2}	mm d^{-1}
S.AFR	Jan	2.2	24.0	13.7	39.9	-117.3	137.2	4.7
S.AFR	Jul	-0.3	39.9	-79.3	-39.7	-144.8	85.1	2.9
IND O.	Jan	3.1	17.1	65.1	85.3	-122.1	188.4	6.5
IND O.	Jul	0.1	32.4	-62.9	-30.4	-130.3	79.9	2.8
AUST	Jan	5.1	26.5	125.3	156.9	-104.4	241.3	8.3
AUST	Jul	0.4	39.4	-63.7	-23.9	-126.1	82.2	2.8
SPCZ	Jan	2.9	-11.0	83.0	74.9	-125.7	180.6	6.2
SPCZ	Jul	-6.8	-20.2	60.5	33.5	-142.8	156.3	5.4
SACZ	Jan	-0.2	4.7	62.1	66.6	-118.0	164.6	5.7
SACZ	Jul	-1.2	20.0	-85.8	-67.0	-136.8	49.8	1.7
SH OTHER	Jan	0.6	10.1	-38.6	-27.9	-133.8	85.9	3.0
SH OTHER	Jul	-1.2	46.1	-110.3	-65.4	-138.1	52.7	1.8
SH TROP	Jan	2.0	12.3	34.1	48.4	-122.6	151.0	5.2
SH TROP	Jul	-1.3	32.0	-71.7	-41.0	-136.2	75.2	2.6
NH TROP	Jan	-0.6	29.5	-38.7	-9.8	-135.1	105.3	3.6
NH TROP	Jul	-1.2	11.9	51.4	62.1	-126.0	168.1	5.8

[1] To get P_o in Wm^{-2}, subtract Q_R and Q_1, then subtract 20 Wm^{-2} from that to account for sensible heating (S_o).
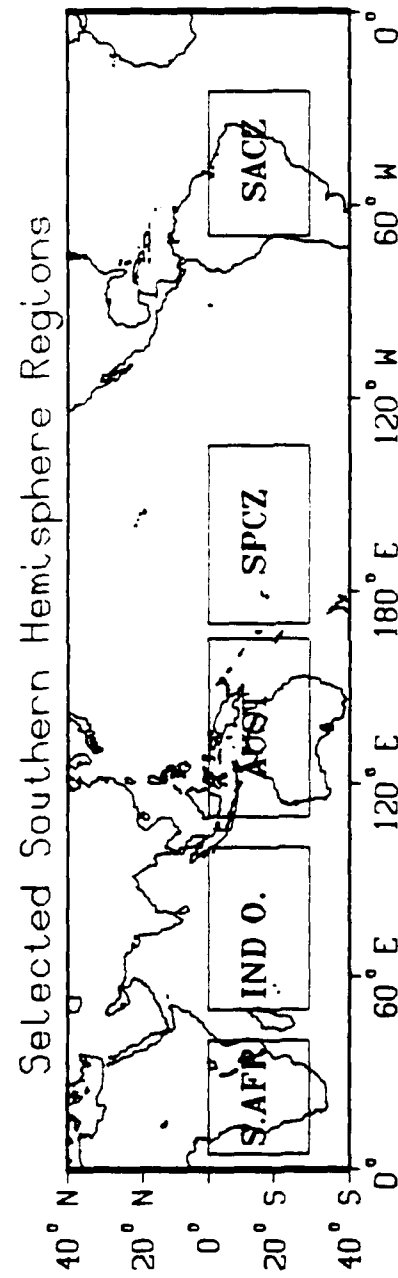
Figure 6. Selected regions in the Southern Hemisphere tropics for computing area averages of terms in the Q_1 budget.

is considerably less than VADS. Positive values of HADS indicate a net advective effect that tends to enhance diabatic heating. Positive values of VADS indicate convectively active regions (rising air). Throughout the Southern Hemisphere VADS is less positive (or more negative) in winter (i.e., July) than in summer, illustrating the more intense convection and increased precipitation that occurs in the summer months. Positive values of Q_1 indicate increased convective activity. Negative values of Q_1 indicate that diabatic cooling processes are dominant. This primarily occurs to the west of South America, which constitutes the major part of the SH Other region. This agrees with the OLR maps (Fig. 5), which show predominantly clear skies in this area.

Wu and Chang (1989) found that large flux divergences or cooling rates are found over anticyclonic areas, and are not associated with intense convective cloud systems. This matches our results quite well since the highest OLR values are over clear anticyclonic areas (e.g., the area west of South America). For each region the highest cooling rate occurs in conjunction with the lowest precipitation rate.

Finally, in Table 1, the P_o values (Q_1 - Q_R - S_o) compare favorably with PV over the oceanic regions, although the comparisons are not as favorable over the continents. However, as noted by PV, radiation values over the continents were suspect; and as noted earlier, radiation estimates are least reliable over land in the present study.

Figures 7 and 8 show typical vertical profiles of s for regions and months which were selected because they illustrate extreme conditions. The figures illustrate how little the monthly average profiles of s vary in the tropics. Australia was the most convectively active and the SH Other region was the least of all the regions studied in January 1986 (Fig. 7). Similar results are seen for the NH Tropics (most active) and SACZ (least active) regions in July 1986 (Fig. 8). At any pressure level the difference in s between regions is less than 1% of the magnitude of s at that level. These profiles
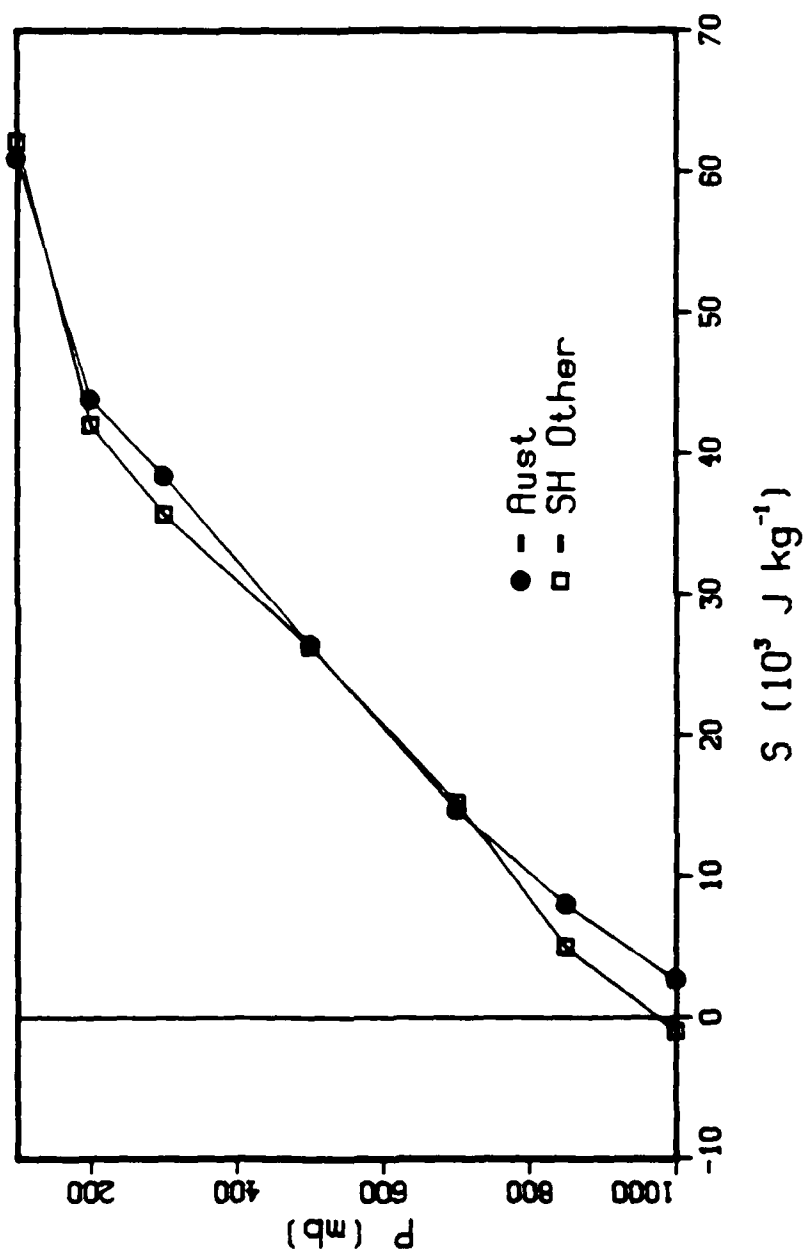
Figure 7. Vertical profiles of dry static energy, s, for AUST and SH Other during January 1986, in 10^3 J kg^{-1}. The abcissa indicates a value of 300 kJ kg^{-1}.
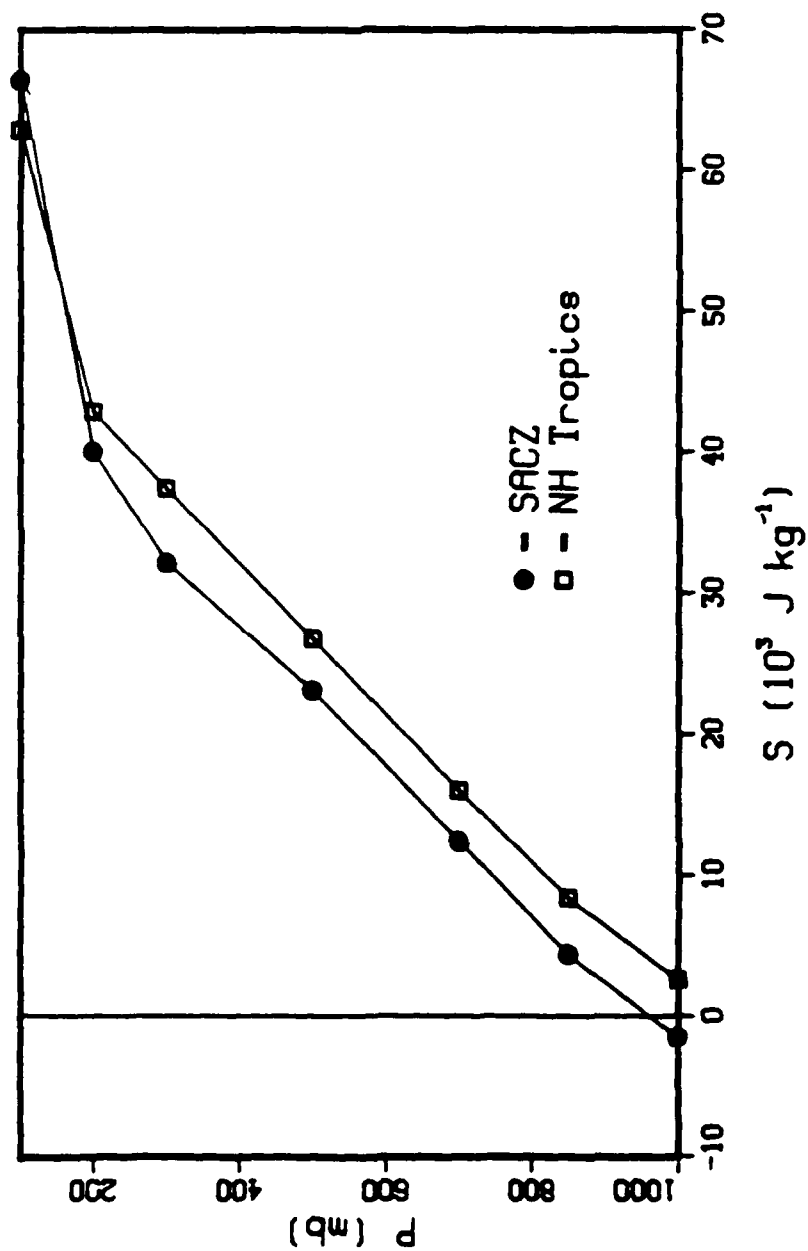
July 1986

Figure 8. Vertical profiles of dry static energy, s, for NH Tropics and SACZ during July 1986, in 10^3 J kg^{-1}. The abcissa indicates a value of 300 J kg^{-1}.

compare favorably with Yanai et al. (1973) and Riehl and Simpson (1979) and show, as theirs did, that the mean dry static energy profile increases quite linearly through the troposphere above the near-adiabatic subcloud layer until reaching the vicinity of the tropopause.

3.2 Hovmoeller Diagrams of Q_1

The Hovmoeller diagrams (Hovmoeller, 1949) presented in this section were computed using 5 day running averages of Q_1 that were latitudinally averaged from 15°S to 15°N. The plots for June 1984 - May 1985 (Fig. 9), June 1985 - May 1986 (Fig. 10), and June 1986 - May 1987 (Fig. 11) are shown with a contour interval of 150 Wm^{-2} and values greater than 150 Wm^{-2} have been shaded. The tick mark for each month on the ordinate axis represents the five day mean centered on the middle of the month.

Several observations can be made when comparing the three years. First of all there is a noticeable increase in the values of Q_1 after May 1985. This is presumably due to the changes in the ECMWF model physics that produced larger values of upper level divergence (see Chapter 1). An analysis of point values shows maximum values of 356, 630, and 513 Wm^{-2} for year 1, year 2, and year 3 respectively. Minimum values were found to be -158, -208, and -229 Wm^{-2}. The variation between years 2 and 3 is only 23% for the maximum values and 10% for the minimum values compared to differences of 77% and 32% between years 1 and 2.

Another prominent difference between years is the shift in maximum values from near 150°E in years 1 and 2 to near 180° throughout most of year 3. Also, there are consistently higher values of Q_1 observed over Central Africa (30°E) during most of year 3 compared to years 1 and 2. The higher values over Central Africa and the eastward shift of the SPCZ in year 3 appear to be linked to the 1986-87
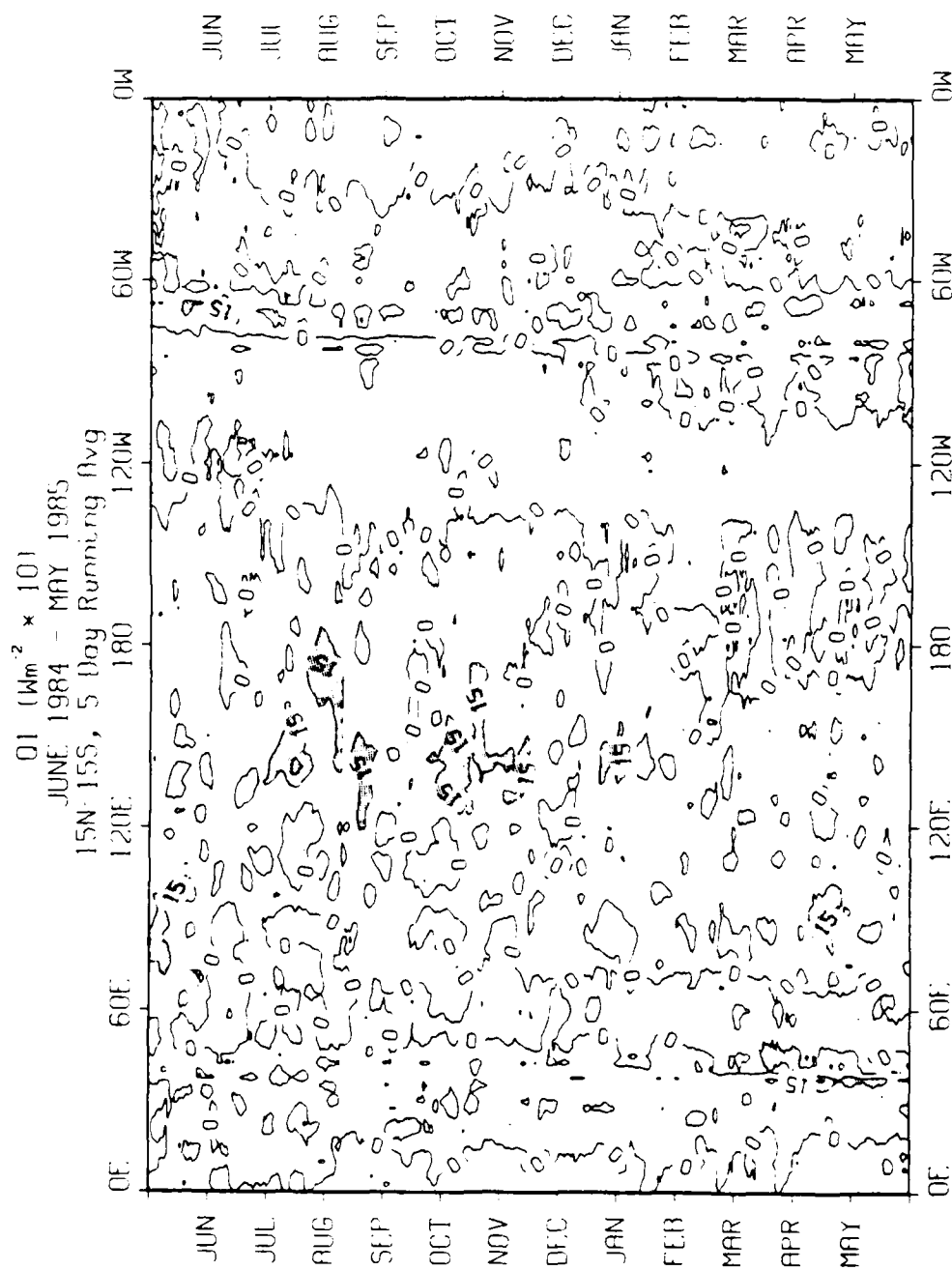
Figure 9. Hovmoeller diagram of Q_1 for June 1984 - May 1985, in Wm^{-2} (values $\geq$ 150 Wm^{-2} are shaded).
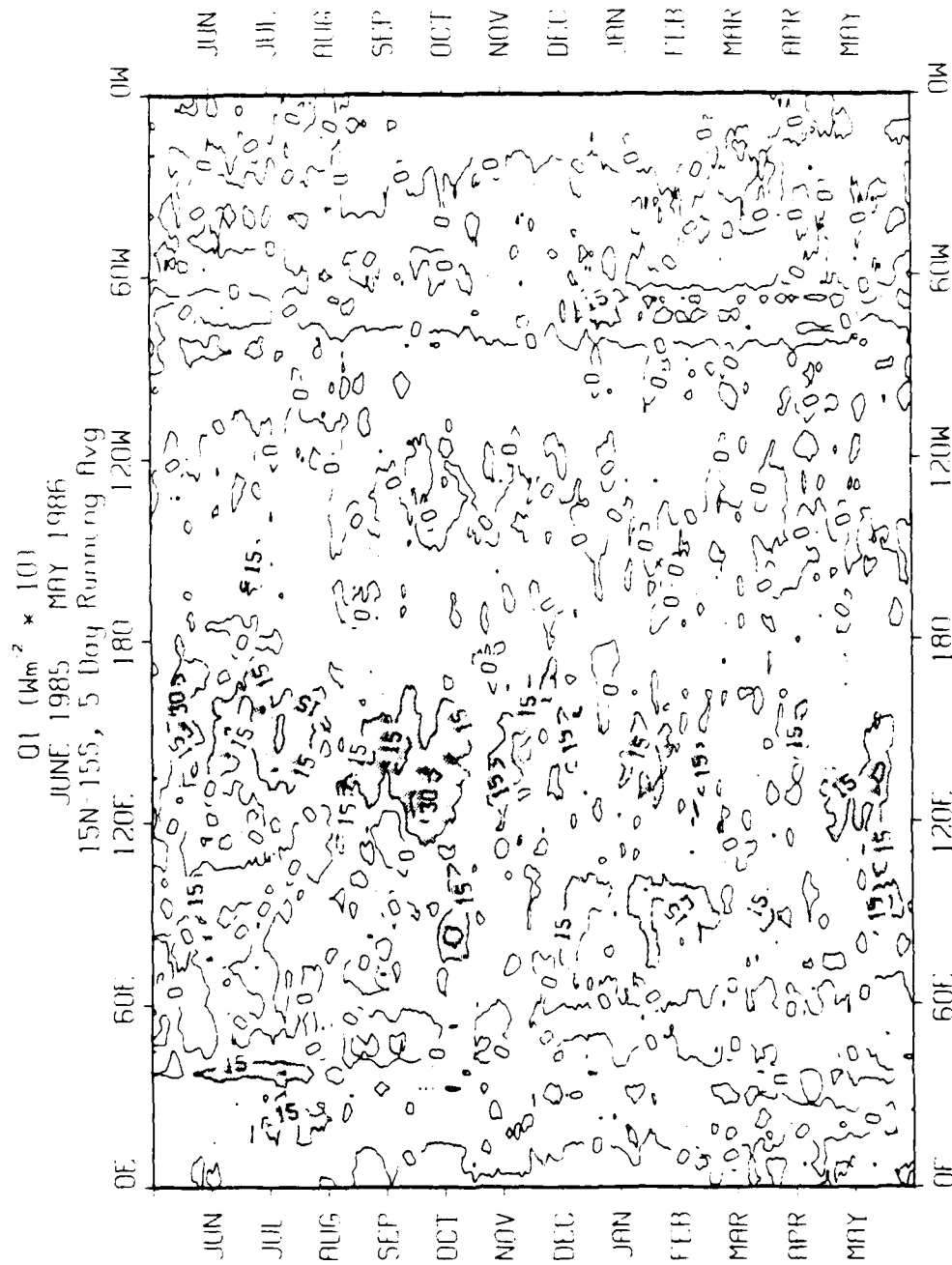
Figure 10. Hovmoeller diagram of Q_1 for June 1985 - May 1986, in Wm^{-2} (values $\geq$ 150 Wm^{-2} are shaded).
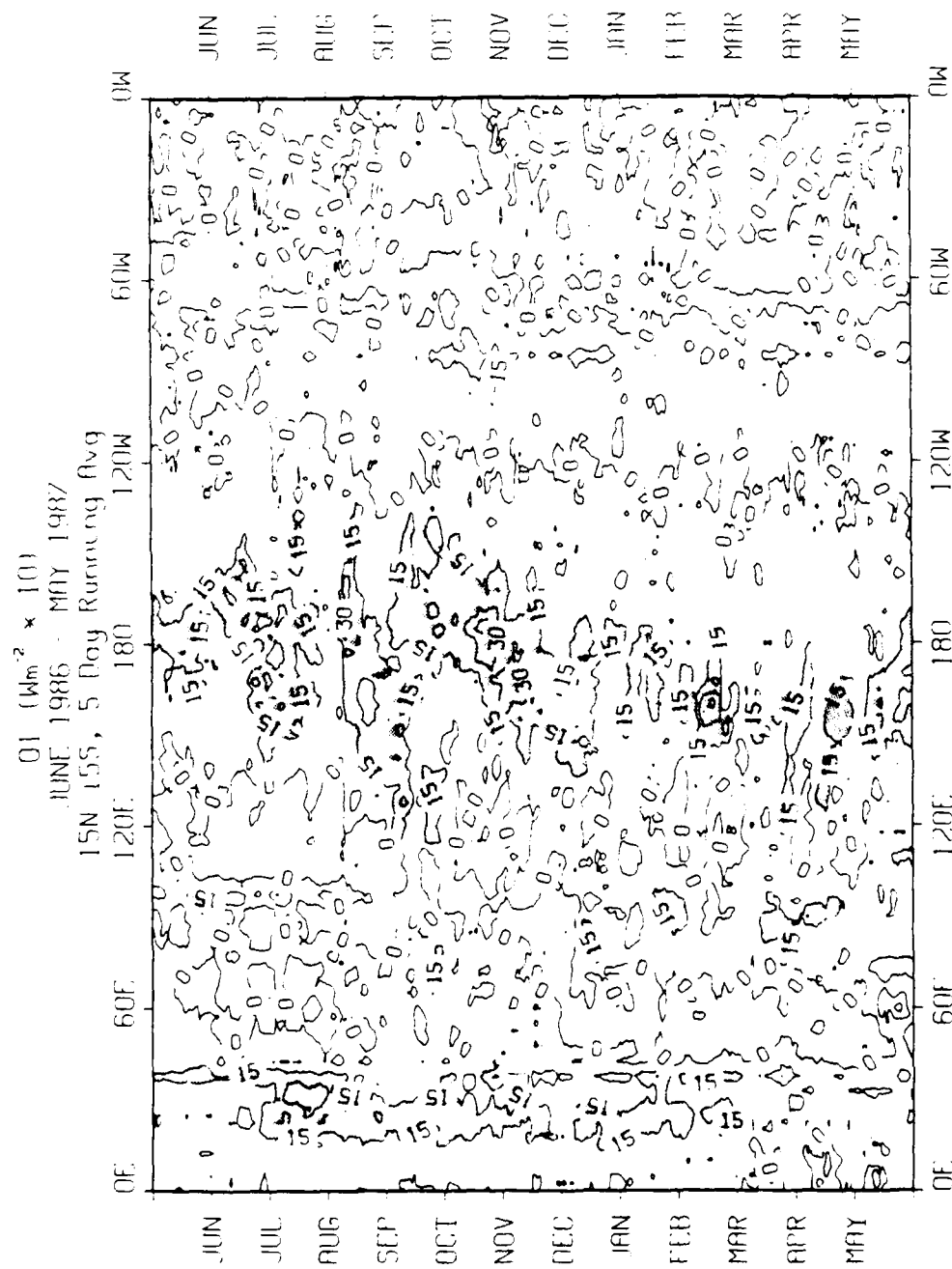
Figure 11. Hovmoeller diagram of Q_1 for June 1986 - May 1987, in Wm^{-2} (values $\geq 150\ Wm^{-2}$ are shaded).

El Nino/Southern Oscillation (ENSO) event (Hendon et al., 1988). It is well known that convection shifts toward the central Pacific during ENSO events (Rasmusson, 1985 and Philander, 1989). Rasmusson notes that the normally prevailing warm sea-surface temperatures (SSTs) in the western tropical Pacific migrate toward the east when an El Nino occurs along the South American coast. This migration of SSTs correlates with an eastward shift in the typical rainfall pattern. For example, during the intense 1982-83 ENSO event a region of enhanced precipitation moved steadily eastward across the Pacific over more than 100° of longitude. The 1986-87 ENSO is a comparatively minor event. Even so, it is apparently linked to the observed shift in Q_1.

Rasmusson (1985) further notes that the central equatorial Pacific appears to be the key region of ocean-atmosphere coupling. The region has SSTs only slightly below the critical threshold (28°C) for widespread convection. Thus, only a slight oscillation in the SST field can shift the west Pacific convergence zone eastward. Combining Rasmusson's observations with those of Lau and Chan (1983), who showed that the central equatorial Pacific was the key center of global teleconnecting weather patterns, provides substantial impetus for further study of the heating and precipitation cycles in the Pacific.

Hendon et al. (1988), in an investigation of the onset of the Australian monsoon, examined data from November 1986 - February 1987 and noted that anomalous convection existed in the central equatorial Pacific until early January 1987. At that time the anomalous ENSO convection diminished rapidly, apparently due to the passage of the descending branch of the 40-50 day oscillation described by Madden and Julian (1971, 1972) and others.

It is not within the scope of the present investigation to conduct an in-depth study of the role of the 40-50 day oscillation in perturbing anomalous precipitation. However, there does appear to be some evidence of this type of temporal fluctuation in

the Q_1 plots during each of the three years. Numerous investigators (e.g., Weickmann et al., 1985) using OLR and upper troposphere circulation features to study the 40-50 day oscillation found the lowest OLR values and hence strongest convection from about 60°E to the Central Pacific. Since Q_1 corresponds to diabatic heating (primarily latent heat release), it is encouraging to see that the results in Figs. 9-11 are in accord with these findings. A more detailed examination of the oscillation is planned for the near future.

Finally, one feature that remained constant was the negative region from approximately 120°W to 60°W, which corresponds to the predominantly clear area off the west coast of South America where diabatic cooling processes dominate.

3.3 Sensitivity Study

VADS is the dominant term in most areas and Trenberth and Olsen (1988a) showed that changes in the ECMWF analysis-forecast system have had their greatest impact on the upper level divergent wind field component and, thus, on tropospheric vertical velocities. To check the sensitivity of the results, random and systematic perturbations were introduced to the ω field. Since VADS = $\omega \, \partial s/\partial p$ and vertical profiles show that $\partial s/\partial p$ is fairly constant, the sensitivity of the term was studied by modifying the original value of ω before VADS was calculated.

All the model changes made from 1980-1986 increased the value of ω. Thus the sensitivity of the results to the ω field was first studied by increasing the original values by 25 and 50% to see what effect systematic magnitude increases would have on the resulting heating and precipitation fields. The results of this test are shown in Table 2. Not surprisingly, a 25% (50%) increase in ω led to approximately a 25% (50%) increase in the value of VADS. However, since the precipitation estimates depend on factors other than VADS, there is a smaller change in P_o. The resulting average change

Table 2. Results of sensitivity study on ω for January 1986. VADS in Wm^{-2}, P_o in mm d^{-1}.

25% Systematic Increase in ω

	VADS Original	VADS Perturbed	Precip Original	Precip Perturbed	Percent Change
S. AFR	13.7	17.8	4.7	4.8	3.0
IND O.	65.1	82.1	6.5	7.1	9.2
AUST	125.3	157.6	8.3	9.4	13.4
SPCZ	83.0	104.0	6.2	6.9	11.8
SACZ	62.1	78.5	5.7	6.3	10.0
SH Other	-38.6	-48.8	3.0	2.6	-12.0
SH	34.1	42.9	5.2	5.5	5.8
NH	-38.7	-47.3	3.6	3.3	-9.1

50% Systematic Increase in ω

	VADS Original	VADS Perturbed	Precip Original	Precip Perturbed	Percent Change
S. AFR	13.7	21.6	4.7	5.0	5.7
IND O.	65.1	99.0	6.5	7.7	18.0
AUST	125.3	189.6	8.3	10.5	26.7
SPCZ	83.0	125.3	6.2	7.7	23.5
SACZ	62.1	94.7	5.7	6.8	19.8
SH Other	-38.6	-58.9	3.0	2.3	-23.3
SH	34.1	51.6	5.2	5.8	11.5
NH	-38.7	-56.9	3.6	3.0	-17.5

Table 2, continued

Perturbed values of VADS, based on random changes in ω.

	VADS Original	$\pm 1\ \mu bar$	$\pm 2\ \mu bar$
S. AFR	13.7	14.1	14.1
IND. O	65.1	66.0	66.6
AUST	125.3	125.9	126.0
SPCZ	83.0	82.5	82.0
SACZ	62.1	63.5	64.6
SH Other	-38.6	-40.0	-41.0
SH	34.1	34.0	33.8
NH	-38.7	-38.4	-39.1

in P_0 was +10% for a 25% increase in ω and a 20% change for a 50% increase. Thus, while P_0 is somewhat sensitive to reasonable systematic errors in ω, it is not overwhelmed by these errors.

To check for the effect of random errors, ω was perturbed using a random number generator. To estimate what the reasonable limits might be for perturbing ω, the spatial mean and standard deviation of ω at 500 mb over the tropical domain were calculated for a 1 day and 5 day time period. In the first case the standard deviation was 0.97 μbar s^{-1} and the second was 0.73 μbar s^{-1}. Thus, ω was perturbed at all the levels using a uniform random distribution of errors ranging from ± 1 μbar s^{-1}. The perturbation was run a second time using ± 2 μbar s^{-1}. In both cases no noticeable difference was seen in the resulting precipitation field and only minor differences were seen in the heating field.

3.4 Annual Precipitation Patterns

This section presents annual precipitation estimates derived using the heat budget technique and compares the results with work done by Dorman and Bourke (1978, 1979, 1981), Dorman (1981), and Jaeger (1976). For brevity, Dorman and Bourke's results will be referred to as DB78, DB79, and DB81. The precipitation estimates for years 1-3 are shown in Fig. 12. Since the Q_1 Hovmoeller diagrams showed a substantial increase from year 1 to year 2, it is no surprise that the annual corresponding increase from year 1 to year 2. In particular the area of > 2 m yr^{-1} covers a much larger area in years 2 and 3 than in year 1.

Since year 1 appeared to be an underestimate of the actual precipitation, only years 2 and 3 were used to form an average annual precipitation map for comparison with Dorman's (1981) 1950-1971 annual average results. The resulting Q_1 map of estimated precipitation shows very similar results to those of Dorman (Fig. 13). The Q_1
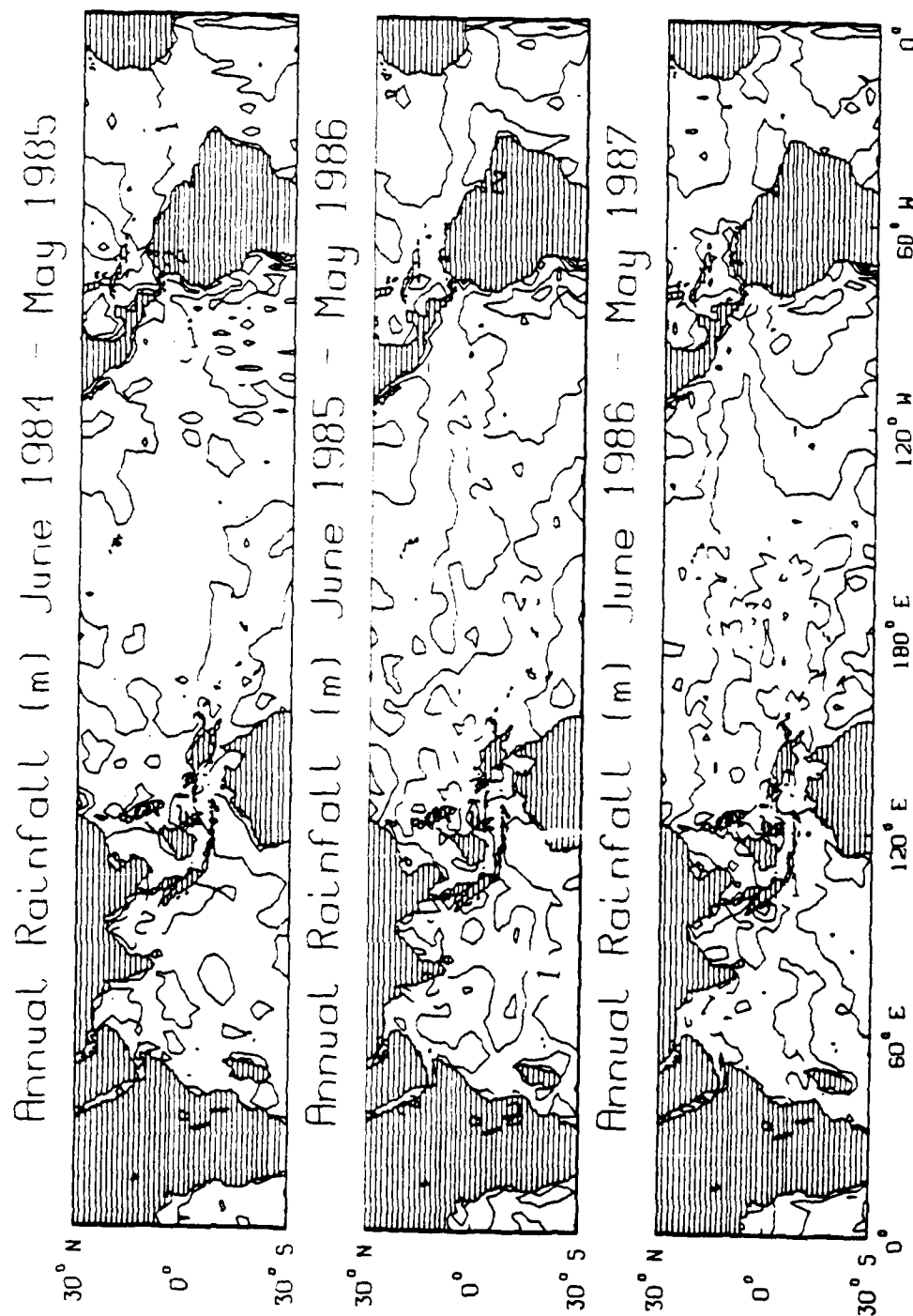
Figure 12. Q_1-budget annual precipitation rate estimates from June 1984 - May 1985, June 1985 - May 1986, and June 1986 - May 1987, in m yr^{-1}.

map of precipitation shows less precipitation off the northeast coast of Australia but the patterns are similar. Particularly good agreement is seen to the southwest of Sumatra (Eq., 100°E), where the 1 and 2 m yr^{-1} contours correspond almost exactly. Fairly good agreement is seen in the South Atlantic, although the Q_1's area of > 2 m yr^{-1} is less than Dorman's. A minimum area is found in both maps off the west coast of South America, and a smaller minimum is seen off the west coast of Australia.

Jaeger's (1976) average annual precipitation, shown in Fig. 14, is offset 180° from the Q_1 maps and covers continental areas, thus visual comparisons are more difficult. However, as with Dorman's (1981) map, precipitation maxima are seen northeast of Australia, and near the island of Sumatra. Jaeger's 3 m yr^{-1} maximum near Australia, while less than Dorman's matches well with the Q_1 results. Overall the Q_1 map and Jaeger's map are remarkably similar. The 2 m yr^{-1} contour extends to about 120°W in both maps. Also, the 1 m yr^{-1} contour off the west coast of South America matches well.

In general, there is quite good agreement between all three estimates of precipitation over the oceanic areas. The problem in determining which one is best occurs because of a lack of "ground truth" measurements over most of the oceans. However, some data are available for comparison. For example, Taylor's (1973) atlas of Pacific island rainfall is based on low island and atoll precipitation measurements and is felt to be representative of the open ocean rainfall. Since this study's grid point precipitation shows a values of precipitation represent an average rainfall amount over a 2.5° by 2.5° grid, two adjacent island stations were frequently averaged for comparison. Table 3 shows a comparison of values from the present study, Dorman (1981), DB79, DB81, and Jaeger (1976). Figure 15 shows the locations of the stations used in Table 3. In the pacific, Taylor's (1973) measurements were used, while the comparisons for the Western and Eastern Atlantic are drawn from work by DB81, who compared their
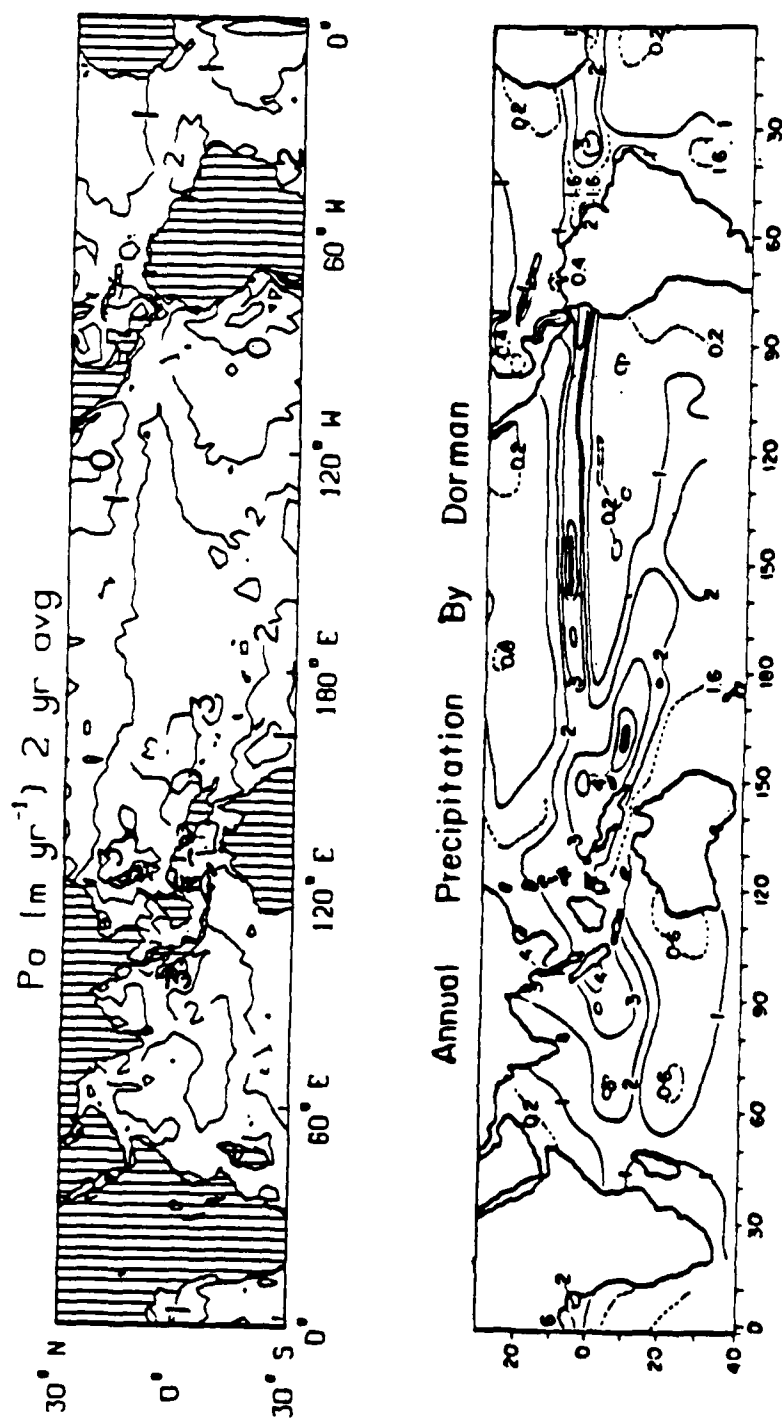
Figure 13. Q_1- budget annual precipitation rate estimate based on June 1985 - May 1987 data shown in comparison to Dorman and Bourke's annual precipitation estimate based on 1951-1961 data in $m\ yr^{-1}$.
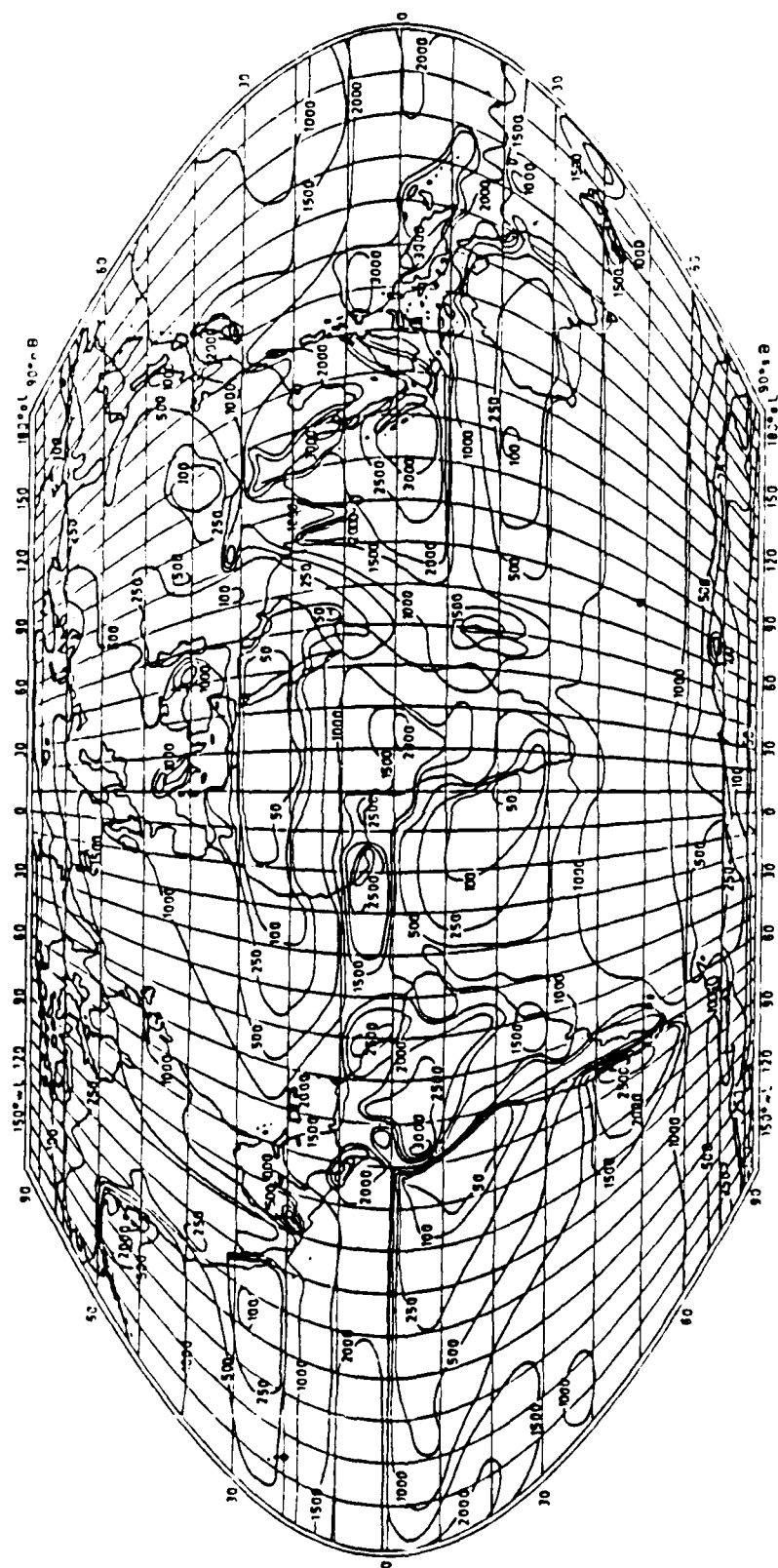
Figure 14. Jaeger's annual precipitation rate estimate in m yr^{-1}.

results with measured coastal and island station rainfall from the Smithsonian World Weather Records for 1951-1960. The estimates for Jaeger's values were made from a careful inspection and extraction of values from his annual precipitation map.

The results for the Q_1 budget are particularly impressive, if one assumes the measured values are correct. The average error between the measured and Q_1-estimated precipitation is approximately -3.6% for all twelve points (range from +15% to -18%). Dorman and Bourke had an average error of -28.2% (range from +22% to -61%) while Jaeger's was -19.2% (range from +119% to -40%). Although this is not a broad enough comparison to claim the Q_1 budget is more accurate than either Jaeger or Dorman and Bourke's methods it appears that over open ocean areas this technique will produce results consistent with observational data. These results also seem good when considering that the Q_1 precipitation estimates are based on a two year mean and then compared to longer means in the other studies.

Although the results are not shown, a more general comparison was made from Smithsonian World Weather Records (1951-60) data, using 30 island and coastal stations in the Atlantic and 20 stations in the Pacific (see DB79 and DB81). For the Pacific region the average Q_1 error was 0.286 m yr^{-1} (23%) compared to DB79's error of 0.267 m yr^{-1} (21%); the mean was 1.26 m yr^{-1}. In the Atlantic the average Q_1 error was 0.641 m yr^{-1} (34%) compared to DB81's 0.890 m yr^{-1} (47%); the mean was 1.89 m yr^{-1}. When averaging all the stations in the Pacific together the measured mean was 1.26 m yr^{-1} compared to Q_1's 1.28 m yr^{-1} (2% error) and DB79's 1.20 m yr^{-1} (5% error). Similar computations in the Atlantic showed a measured mean of 1.89 m yr^{-1} compared to Q_1's 1.46 m yr^{-1} (23% error) and DB81's 1.00 m yr^{-1} (47% error). Combining both regions gave a measured mean of 1.64 m yr^{-1} compared to Q_1's estimate of 1.39 m yr^{-1} (15% error) and Dorman and Bourke's 1.08 m yr^{-1} (34% error). Thus, the Q_1 method seems to represent an improvement over Dorman and Bourke's method. The errors are

Table 3. Island and coastal station data compared with Q_1-budget
precipitation estimates in mm d^{-1}.

Point	Area	Stations used	Lat.	Long.
1	Central Pacific	Penrhyn	9°S	158°W
		Puka Puka	11°S	165°W
2	Central Pacific	Fanning	4°N	160°W
		Washington	4°N	160°W
3	Central Pacific	Kapingamarangi	1°N	154°E
4	Central Pacific	Mokil	6°N	159°E
5	Western Atlantic	Maiquetia	11°N	67°W
		Guiria	11°N	62°W
6	Western Atlantic	Belize	17°N	88°W
		Swan Island	17°N	84°W
7	Western Atlantic	Olinda	8°S	35°W
		Salvador	13°S	38°W
8	Western Atlantic	Turiacu	23°S	43°W
9	Eastern Atlantic	Harbel	6°N	10°W
10	Eastern Atlantic	Libreville	0°S	9°E
11	Eastern Atlantic	Mayumba	3°S	11°E
12	Eastern Atlantic	Adiake	5°N	3°W
		Contou	6°N	2°E

Point	Annual rainfall (mm) Measured[1]	Q_1	Dorman[2]	Jaeger
1	2373	2208	1250	1500
2	2492	2535	5050	2050
3	2808	3228	3000	2250
4	2056	2907	3000	2250
5	730	827	625	1600
6	1524	1711	1000	1500
7	1661	1766	950	1000
8	2092	1715	1000	1250
9	3386	2783	2150	3000
10	3095	2739	1200	1900
11	1745	1480	1250	2000
12	2013	2095	900	1500
Average	2248	2167	1615	1817

[1] Taylor (1973) used for points 1-4, Smithsonian data for points 5-12.
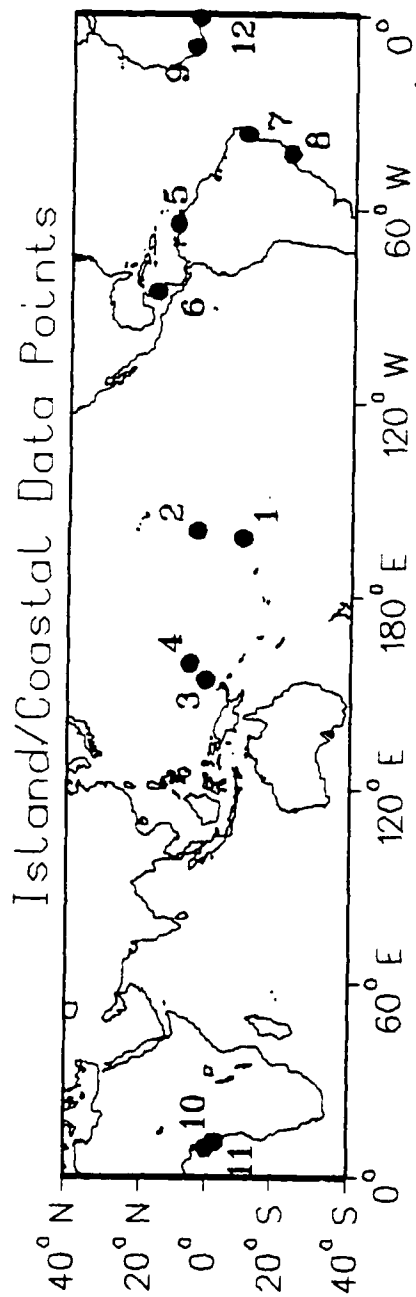[2] DB79 used for points 1-4, DB81 for points 5-12.

Figure 15. Island and coastal station data points compared with Q_1 estimated precipitation rates.
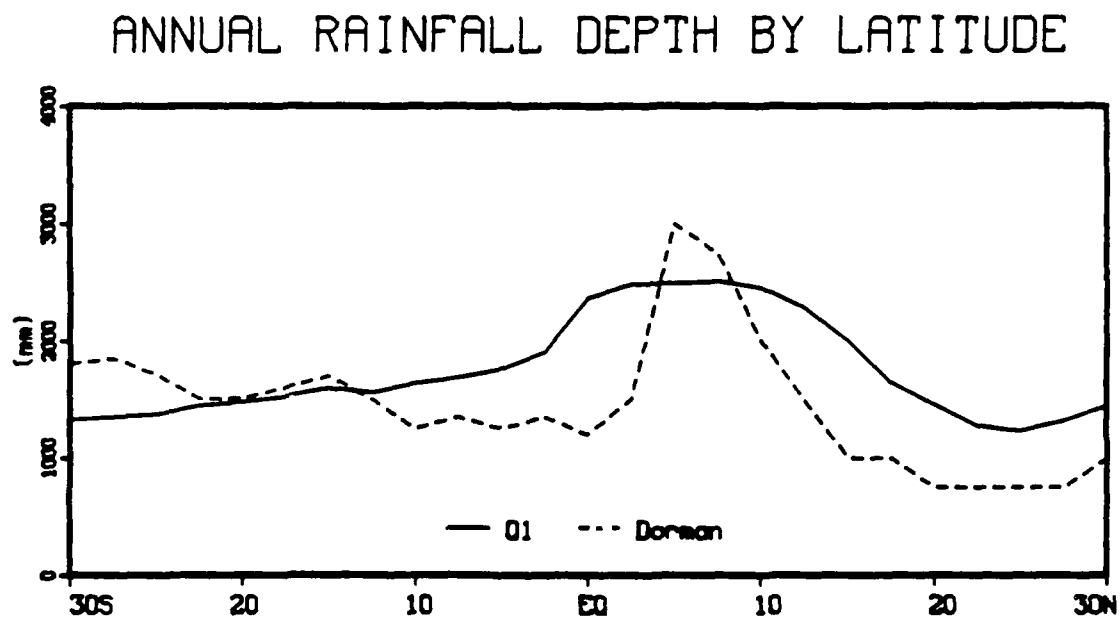
Figure 16. Comparison of Q_1-budget and Dorman and Bourke's annual latitudinally averaged precipitation rate in mm d^{-1}.

higher for both methods in the larger comparisons since the coastal stations include orographic effects which are beneath the resolution of the averaging techniques used.

For further comparison, latitudinally and annually averaged rainfall over the Pacific is shown together with DB78's results (Fig. 16). It is immediately apparent that Q_1 presents a smoother estimate than DB79. The smoothness of the Q_1 plot is not too surprising since the use of objective analyses probably precludes the identification of maximum peaks similar to that presented by DB79. The difference may also be due to lack of adequate data by DB79. Their estimate of precipitation across the equatorial Pacific is based mainly on less than 500 observations per 2° by 5° rectangle over a 22 year period (1950-1971). This equates to less than 23 observations per year and it is possible that DB79's estimate is biased. Overall, the trends are similar, with maxima and minima occurring in roughly the same regions. The Q_1 latitudinal mean was 1745 mm d^{-1} compared to 1453 mm d^{-1} for DB79. This is consistent with the results obtained in the station analyses, which showed DB79 and DB81 to underestimate the measured precipitation.

3.5 Monthly Precipitation Patterns

In this section latitudinally averaged results, similar to those presented for an annual comparison, are presented for January and July. Also, the 36 monthly precipitation rate maps (June 1984-May 1987) which are shown in the Appendix are discussed in this section. The maps in the Appendix are presented in sets of three to conserve space and to allow for easier seasonal comparisons over the period of study.

Figure 17 presents latitudinally averaged rainfall over the Pacific and compares the Q_1 estimate with DB78's estimate. For January, the Q_1 estimate is slightly less than Dorman and Bourke's (153 versus 157 mm d^{-1}). In July, the opposite is true, the Q_1 estimate is more than Dorman and Bourke's (146 versus 103 mm d^{-1}). Overall the

trends are similar with the biggest discrepancy being seen in the Southern Hemisphere during January. Part of the difference is no doubt due to the different analysis techniques as noted with respect to Fig. 16.

The precipitation maps in the appendix show a few noteworthy features. First, note that the first year's maps reflect lower precipitation rates than the last 2 years, presumably due to changes in the model physics made at ECMWF in May 1985. For example, the summer of 1984 shows contour levels of 3 mm d^{-1} over most of the domain, while the summers of 1985 and 1986 show large areas of 6 mm d^{-1}.

The precipitation rates follow the expected annual migration with maximum activity in the Southern Hemisphere (Northern Hemisphere) during December-March (June-September). However, December 1986-February 1987 stands out as an especially active time for the SPCZ region. Contours of 12 mm d^{-1} are seen in each month. This contrasts sharply with December 1985-February 1986 when contours of 6 mm d^{-1} are typical. The reason for this is thought to be the existence of the previously mentioned ENSO event in 1986-87 (see Chapter 3.2).

The appendix maps are mainly included for their reference value. This technique may be valuable in creating monthly rainfall maps for use in the calibration phase of the upcoming Tropical Rainfall Measuring Mission (TRMM). Also, maps of the diabatic heating fields (not shown) can easily be produced and may be of value in modeling work.

The information presented in the appendix maps is more easily grasped if the values are averaged for a region and presented as a time-series plot. Thus, the next section presents regional averages and trend information.

JANUARY RAINFALL DEPTH BY LATITUDE
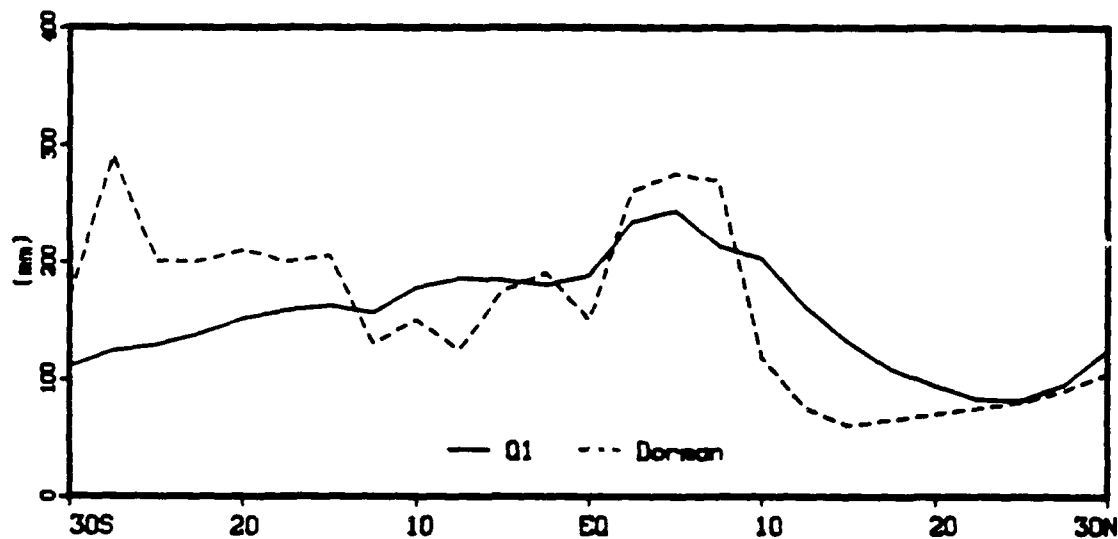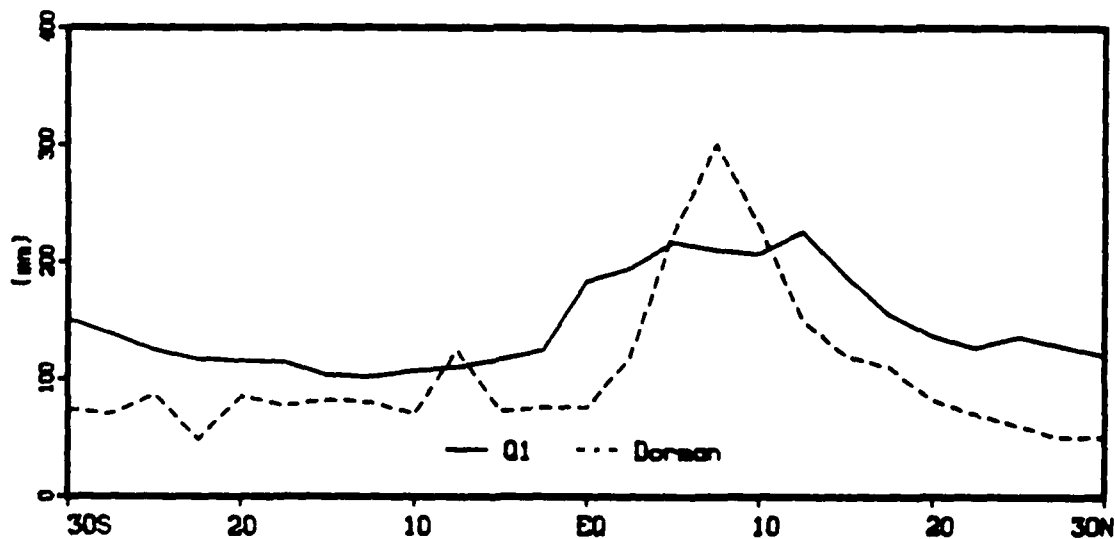
JULY RAINFALL DEPTH BY LATITUDE

Figure 17. Comparison of Q_1-budget and Dorman and Bourke's January and July latitudinally averaged precipitation rates in mm d^{-1}.

3.6 Regional Precipitation Patterns

This section presents monthly mean time series for selected regions in the tropics. The SPCZ with an average annual precipitation rate of 6.09 mm d^{-1} is the most convectively active region (based on the last 2 years of data). Normalizing the regional data by setting SPCZ = 1 yields the following:

SAFR = 0.77	SPCZ = 1.00	SH = 0.65
IND O. = 0.69	SACZ = 0.67	NH = 0.77
AUST = 0.73	SH Other = 0.46	TROP = 0.71

This clearly indicates the importance of the SPCZ to the global hydrological cycle, at least for the June 1985-May 1987 period. Figures 18 and 19 display time series plots of precipitation in mm d^{-1} for the 36 months of the study. The trend line (using the least squares method) is also dashed in for the last 2 years of each region. All of the selected Southern Hemisphere regions show a maximum rainfall rate during the Southern Hemisphere summer (Dec.-Feb.) when convective activity is at its peak. Although this presents no surprises, it does reinforce confidence in the results since they reflect well known precipitation patterns. Further, as expected, the SH and NH are almost exactly out of phase. The slight, but insignificant, increase seen in the tropical precipitation plot (TROP) is probably a result of the model changes that occurred over the period of study.

The trend information is now presented in tabular form to aid in the interpretation of the time series plots.
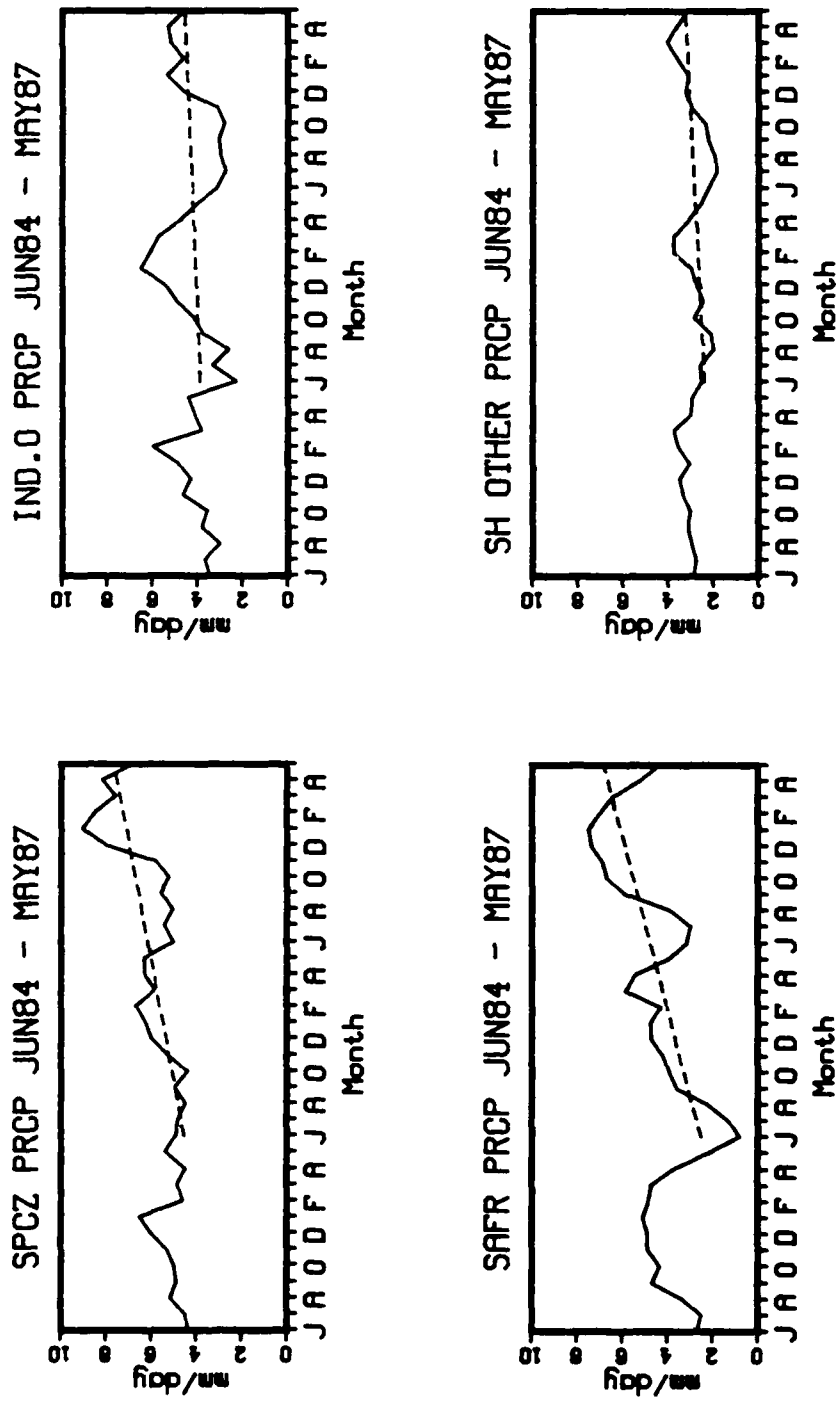
Figure 18. Time series of area-averaged precipitation rates (mm d⁻¹) for SPCZ, IND O., SAFR, and SH Other for June 1984 - May 1987.
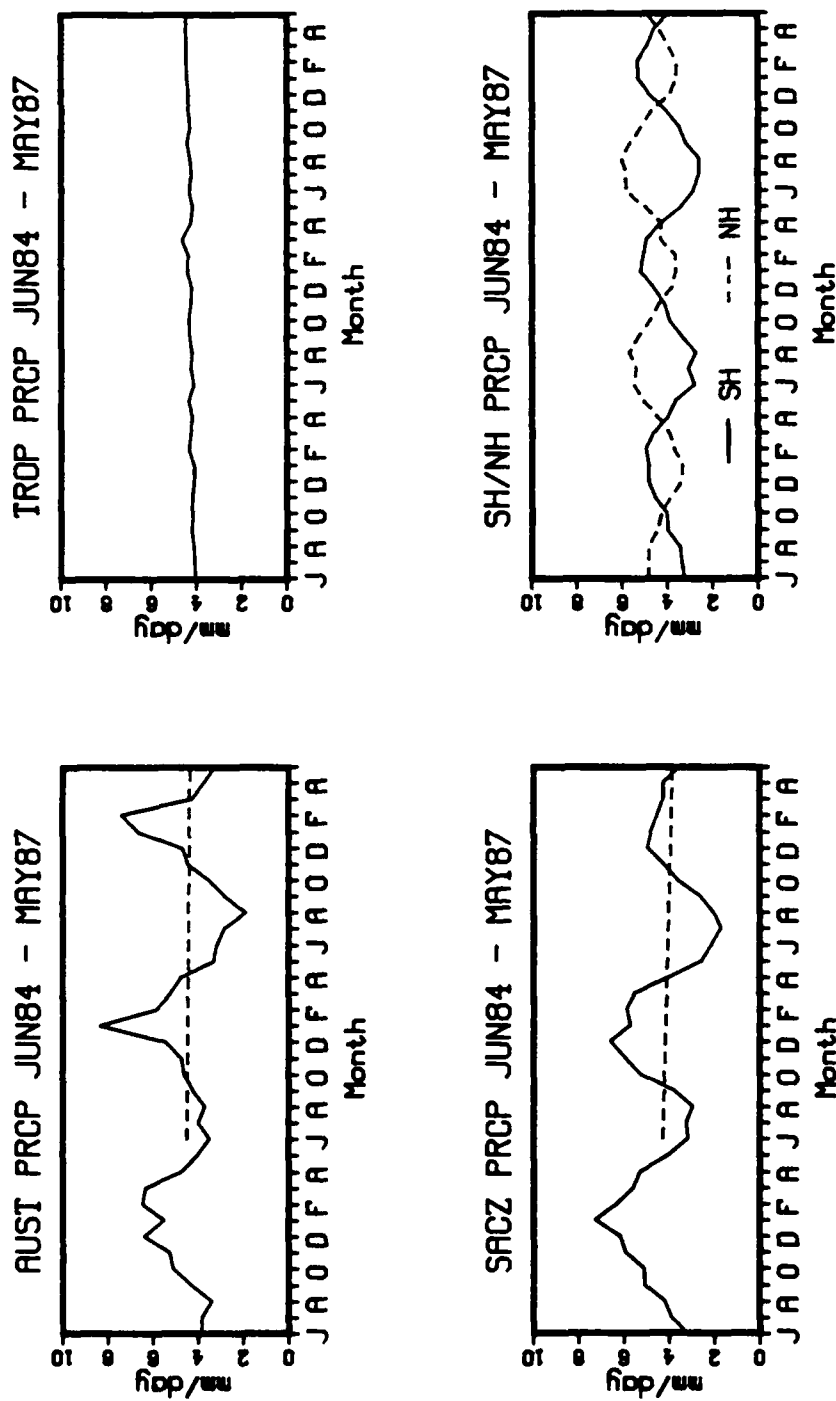
47

Figure 19. Time series of area-averaged precipitation rates (mm d⁻¹) for AUST, TROP, SACZ, and SH/NH for June 1984 - May 1987.

Table 4. Average rainfall rate (mm d^{-1}) and trend, in terms of slope, (mm d^{-1} m^{-1}) for selected regions during years 2 and 3.

Region	Average rainfall	Slope	Region	Average rainfall	Slope
SAFR	4.67	0.187	SH Other	2.81	0.038
IND O.	4.21	0.030	SH	3.97	0.047
AUST	4.50	-0.007	NH	4.70	-0.029
SPCZ	6.09	0.136	TROP	4.33	0.009
SACZ	4.05	-0.020			

Several features seen in the trend data may be worthy of further study. First, there is a strong trend toward increasing precipitation rates over the last 24 months in the SPCZ and SAFR regions, while other regions show weaker positive or negative trends. Overall, rainfall in the SH tropics increased only slightly, thus there appears to have been a shift in the tropical circulation patterns during the 2-year period. Also, the NH tropics appear to have undergone a slight decrease in the amount of rainfall received. A longer period of data needs to be analyzed before any definite conclusions can be drawn; however, it should be remembered that model changes before May 1985 make comparisons difficult when ECMWF analyses are used.

AUST shows a sharp peak near mid-summer of each year that correlates with the observed monsoon season there. Hendon et al. (1988) notes that the monsoon season accounts for up to 75% of the annual rainfall over northern Australia.

Another notable feature is the greater annual variation in the SH than the NH. This variation increases with time, presumably due to model changes in the analysis of the divergent wind field. For example, in July 1984 the difference between SH and NH rainfall was 1.4 mm d^{-1}, while in July 1985 and July 1986 it was 2.3 and 3.2 mm d^{-1}, respectively. There is also a steady increase in the January rainfall difference although it is not as great. When the SH and NH precipitation rates are averaged together the

resulting TROP plot shows no annual or seasonal variation. Thus, it appears that the tropics as a whole represent a fairly constant latent heat source for the atmosphere.

4 SUMMARY AND RECOMMENDATIONS

4.1 Summary

The primary goal of this study was to discover if the "apparent" heat source (Q_1) budget technique is a viable method for calculating tropical oceanic precipitation using a routinely available data set. Q_1 was calculated as the total derivative of dry static energy following the development of Yanai et al. (1973). It was computed at standard pressure levels using the WMO archive version of the ECMWF data set and then set equal to the sources and sinks of diabatic heating. Latent heating and sensible heat transfer from the ocean to the atmosphere were seen as sources while radiative cooling was seen as a sink. Sensible heating was assumed to have a constant value of 20 Wm^{-2} based on the studies of PV and others. The net radiation was calculated from monthly OLR values and assumed values of 70 Wm^{-2} for absorbed shortwave radiation and 50 Wm^{-2} for net longwave radiation from the surface.

Maps showing the contribution to the Q_1-budget by its individual terms were presented for January and July 1986. Overall, the VADS term dominates, while the DSDT term was negligible.

Hovmoeller diagrams of five-day running means of Q_1 were examined for the 36 months of the study. The effects of the 1986-1987 El Nino were seen in the eastward shift of the maximum diabatic heating field from about 150°E to 180°. Some evidence of the 40-50 day oscillation was inferred although this remains a potential area for future study.

Since the dominant component of Q_1 was VADS, a sensitivity study was done by systematically and randomly perturbing ω. When ω was systematically perturbed by 25% (50%) the resulting changes in the heating field were 25% (50%) but only 10% (20%) in the precipitation field. When ω was randomly perturbed by up to 2 μbars s^{-1} the resulting heating field was only minimally affected and the precipitation field was not affected.

Annual precipitation maps were presented and compared with annual average maps from work by Jaeger, Dorman and Bourke, and Dorman as well as limited island and coastal station data (Taylor's atlas and Smithsonian World Weather Records). The results from this study compared favorably with previous estimates and show an average error of 15% when compared to a ten year annual average of 50 observed island and coastal stations. In addition, precipitation estimates were latitudinally averaged and compared to Dorman and Bourke's results for January and July and to Dorman's results for annual precipitation. Maps for all 36 months of the period of study are shown in the appendix.

In the final section, time series of regionally averaged precipitation were shown. The plots were discussed with regard to spatial and temporal variations. The trend over the last 24 months of the study was also shown and discussed. The SPCZ region was the most convectively active region, while the SH Other region was the least active. Overall the SH increased in the amount of precipitation received while the NH decreased. The tropics as a whole showed no annual or seasonal variation and, thus, seem to represent a fairly constant latent heat source for the atmosphere.

4.2 Recommendations

The results of this study indicate that the heat budget technique can be used successfully to estimate open ocean rainfall rates. These estimates could be made even

better, however, if reliable estimates of sensible heating and the radiation components were available. Therefore, it is recommended that increased effort be devoted to achieving better parameterization schemes for these important quantities.

As demonstrated by numerous investigators the central equatorial Pacific is a key region in directing global weather patterns. Much more work needs to be done to gain a better understanding of tropical circulation features over the Pacific. As noted in section 3.2 for example, there appears to be some evidence of the 40-50 day oscillation in the diabatic heating fields. Band-pass filtering and other statistical techniques outside the scope of this research should be applied to the data to determine if there are any significant temporal variations present.

As Trenberth and Olsen (1988c) have suggested, the only way to determine any long term trends in the tropics is to reanalyze the original data gathered before May 1985 with the current version of the ECMWF model. As seen in the monthly precipitation maps, and in the time-series plots presented, the changes made at that time preclude any meaningful comparison with data analyzed before May 1985. The El Nino event of 1982-1983 would make a particularly interesting study of the changes in the diabatic heating and resulting precipitation fields, using the Q_1-budget technique if improved analyses were available.

Also, a more detailed comparison of the Q_1 precipitation estimates should be made using the analyses since May 1985. This would perhaps generate further insight into where the precipitation estimates are the most reliable.

Finally, this study suggests that the diabatic heating fields and precipitation rates generated by the Q_1 technique hold great potential as an inexpensive calibration tool for satellite precipitation (e.g., the upcoming Tropical Rainfall Measuring Mission, TRMM, project) measurements over the tropics.

LIST OF REFERENCES

LIST OF REFERENCES

Arakawa, A. and W.H. Schubert, 1974: Interaction of cumulus cloud ensemble with the large-scale environment, Part I. J. Atmos. Sci., **31**, 674-701.

Arkin, P.A. and B.N. Meisner, 1987: The relationship between large-scale convective rainfall and cold cloud over the western hemisphere during 1982-84. Mon. Wea. Rev., **115**, 51-74.

Battan, L.J., 1973: Radar Observation of the Atmosphere, The University of Chicago Press, Chicago, Ill., 104-113.

Betts, A.K. and W. Ridgway, 1988: Coupling of the radiative, convective, and surface fluxes over the equatorial pacific. J. Atmos. Sci., **45**, 522-536.

Chou, M.D., 1985: Surface radiation in the tropical pacific. J. Climate Appl. Meteor., **24**, 83-92.

Dorman, C.E., 1981: Ground truth for oceanic rainfall. Precipitation Measurements from Space, Workshop Report, NASA, Goddard Laboratory for Atmospheric Sciences.

Dorman, C.E. and R.H. Bourke, 1978: Maps of Pacific rainfall. Technical Report 78-2, Center for Marine Studies, San Diego State University.

_____ and _____, 1979: Precipitation over the Pacific Ocean, 30°S to 60°N. Mon. Wea. Rev., **107**, 896-910.

_____ and _____, 1981: Precipitation over the Atlantic Ocean, 30°S to 70°N. Mon. Wea. Rev., **109**, 554-563.

Emanuel, K.A., 1988: Toward a general theory of hurricanes. Am. Sci., **76**, 370-379.

Flueck, J.A., 1981: Some statistical problems inherent in measuring precipitation. Precipitation Measurements from Space, Workshop Report, NASA, Goddard Laboratory for Atmospheric Sciences.

Frank, W.M., 1983: The cumulus parameterization problem. Mon. Wea. Rev., **111**, 1859-1871.

Garstang, M., 1967: Sensible and latent heat exchange in low latitude synoptic scale systems. Tellus, **19**, 492-508.

Geiger, R., 1965: Wandkarten 1:30 Mill., Jahrlicher Niederschlag. Perthes Verlag, Darmstadt.

Gruber, A., M. Varnadore, P.A. Arkin, and J.S. Winston, 1986: Monthly and seasonal mean outgoing longwave radiation and anomalies. NOAA Tech. Report, NESDIS 26, 243 pp.

Gupta, S.K., 1989: A parameterization for longwave surface radiation from sun-synchronous satellite data. J. Climate, 2, 305-320.

Heddinghaus, T.R. and A.F. Kruger, 1981: Annual and interannual variations in outgoing longwave radiation over the tropics. Mon. Wea. Rev., 109, 1208-1218.

Hendon, H.H., N. Davidson, and B. Gunn, 1988: Australian summer monsoon onset during AMEX 1987. Mon. Wea. Rev., 117, 370-390.

Holton, J.R., 1979: An Introduction to Dynamic Meteorology, 2nd ed. Academic Press, New York.

Hovmoeller, E., 1949: The trough-and-ridge diagram. Tellus, 1, 62-66.

Jaeger, L., 1976: Monatskarten des niederschlags fur die ganze erde. Berichte des Deutschen Wetterdienstes, Nr 139 (Band 18). Offenbach a. M., 38 pp. and plates.

Kuo, H.L., 1965: On the formation and intensification of tropical cyclones through latent heat release by cumulus convection. J. Atmos. Sci., 22, 40-63.

_____, 1974: Further studies of the parameterization of the influence of cumulus convection on large scale flow. J. Atmos. Sci., 31, 1232-1240.

Lau, K. and P.H. Chan, 1983: Short term climatic variability and atmospheric teleconnections from satellite-observed outgoing longwave radiation. Part 1: Simultaneous relationships. J. Atmos. Sci., 40, 2735-2750.

Madden, R.A. and P.R. Julian, 1971: Detection of a 40-50 day oscillation in the zonal wind in the tropical pacific. J. Atmos. Sci., 28, 702-708.

_____ and _____, 1972: Description of global-scale circulation cells in the tropics with a 40-50 day period. J. Atmos. Sci., 29, 1109-1123.

Manabe, S., J.Smagorinsky, and R.F. Strickler, 1965: Simulated climatology of a general circulation model with a hydrological cycle. Mon. Wea. Rev., 93, 769-798.

McBride, J.L., 1981: An analysis of diagnostic cloud mass flux models. J. Atmos. Sci., 38, 1977-1990.

Middleton, W.E.K., 1969: Invention of Meteorological Instruments, Johns Hopkins Press, Baltimore, MD.

Miller, B.L. and D.G. Vincent, 1987: Convective heating and precipitation estimates for the tropical South Pacific during FGGE, 10-18 January 1979. Quart. J. Roy. Meteor. Soc., 113, 189-212.

Mintz, Y., 1981: A brief review of the present status of global precipitation estimates. Precipitation Measurements from Space, Workshop Report, NASA, Goddard Laboratory for Atmospheric Sciences.

Newell, R.E., J.W. Kidson, D.G. Vincent, and G.J. Boer, 1974: The General Circulation of the Tropical Atmosphere and Interactions with Extratropical Latitudes. Vol. 2, The M.I.T. Press, Cambridge, MA.

Pedigo, C.B. and D.G. Vincent, 1990: Tropical precipitation rates during SOP-1, FGGE, estimated from heat and moisture budgets. Mon. Wea. Rev. (to appear in Mar. 90).

Peng, L., M.D. Chou, and A. Arking, 1982: Climate studies with a multilayer energy balance model. Part I: Model description and sensitivity to the solar constant. J. Atmos. Sci., 39, 2639-2656.

Philander, G., 1989: El Nino and la nina. Am. Sci., 77, 451-459.

Rao, N.J., A.S. Mascarenhas, and Y. Yamazaki, 1980: Air-sea interaction studies at the station occupied by R/V Sirius. Boundary-Layer Meteorol., 19, 387-391.

Rasmusson, E.M., 1985: El Nino and variations in climate. Am. Sci., 73, 168-177.

Riehl, H. and J.S. Simpson, 1979: The heat balance of the equatorial trough zone revisited. Contributions to Atmos. Physics, 52, 287-305.

Schott, G., 1926: Geographie des Atlantischen Ozeans Boysen Verlag, Hamburg.

Supan, A., 1898: Die Jahrlichen Niederschlagsmengen auf der Meeren. Petermanns Geogr. Mitt., 44, 179-182.

Taylor, R.C., 1973: An Atlas of Pacific Island Rainfall. Report HIG-73-9, Hawaii Institute of Geophysics, 7 pp + 13 figs.

Thompson, R.M., Jr., S.W. Payne, E.E. Recker, and J.S. Reed, 1979: Structure and properties of synoptic scale wave disturbances in the Intertropical Convergence Zone of the eastern Atlantic. J. Atmos. Sci., 36, 53-72.

Trenberth, K.E. and J.G. Olsen, 1988a: An evaluation and intercomparison of global analyses from the National Meteorological Center and the European Centre for Medium Range Weather Forecasts. Bull. Am. Meteor. Soc., 69, 1047-1057.

_____ and _____, 1988b: ECMWF global analyses 1979-1986: circulation statistics and data evaluation. NCAR Tech. Note, NCAR/TN-300 + STR 94 pp and 12 fiche.

Trenberth, K.E. and J.G. Olsen, 1988c: Intercomparison of NMC and ECMWF global analyses: 1980-1986. NCAR Tech. Note, NCAR/TN-301 + STR 81 pp.

Tucker, G.B., 1961: Precipitation over the North Atlantic Ocean, Quart. J. Roy. Meteor. Soc., 87, 147-158.

Wallace, J. M. and P.V. Hobbs, 1977: Atmospheric Science, Academic Press, New York, 316-322.

Weickmann, K.M., G.R. Lussky, and J.E. Kutzbach, 1985: Intraseasonal (30-60 day) fluctuations of outgoing longwave radiation and 250 mb streamfunction during northern winter. Mon. Wea. Rev., 113, 941-961.

Wu, M.C. and C. Cheng, 1989: Surface downward flux computed by using geophysical parameters derived from HIRS 2/MSU soundings. Theor. and Appl. Climo., 40, 37-51.

Yanai, M., S. Ebensen, and J.H. Chu, 1973: Determination of the bulk properties of tropical cloud clusters from large-scale heat and moisture budgets. J. Atmos. Sci., 30, 611-627.

APPENDIX
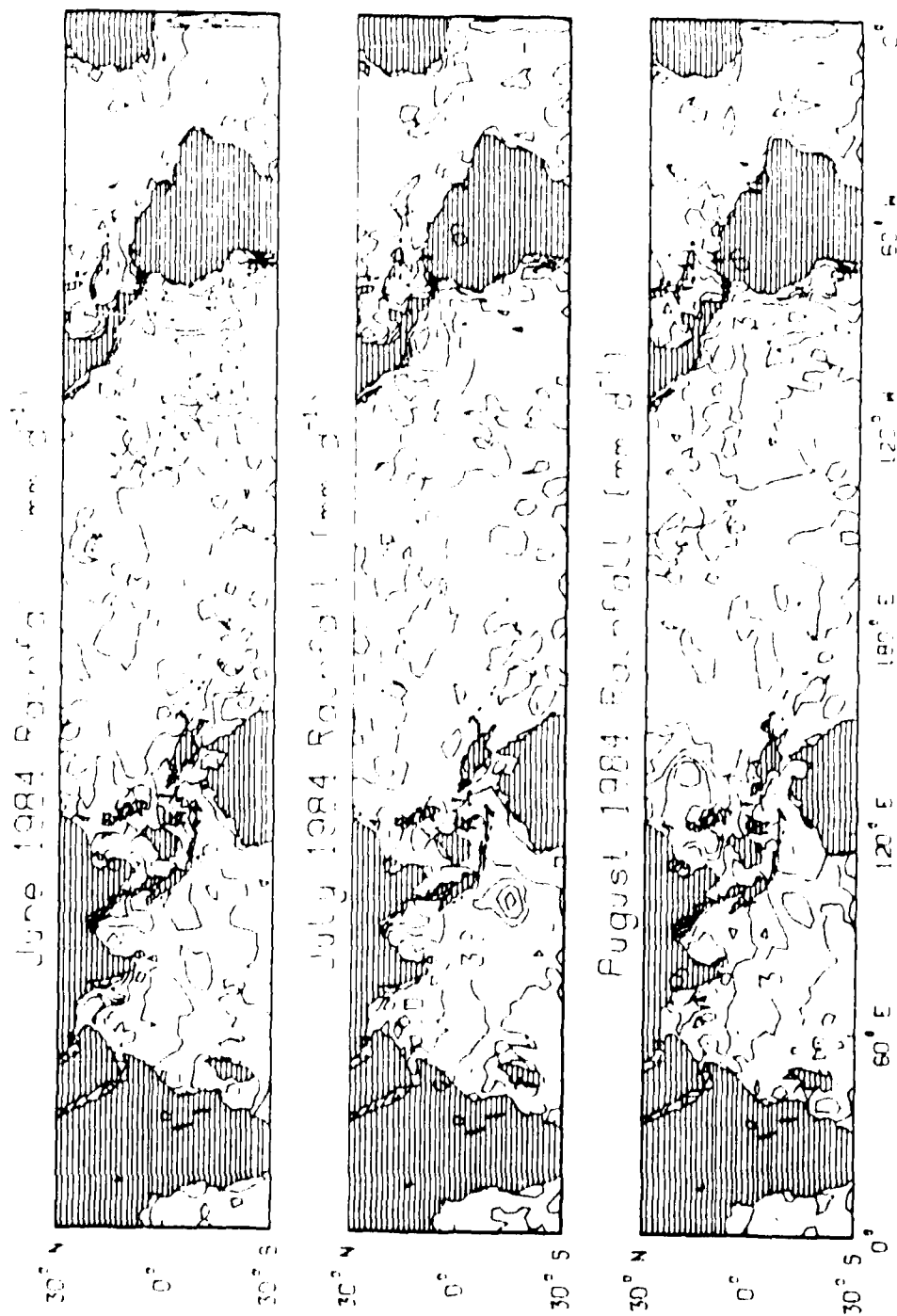
Figure A.1 Q_1 precipitation rate estimate for June, July and August 1984 in mm d^{-1}.
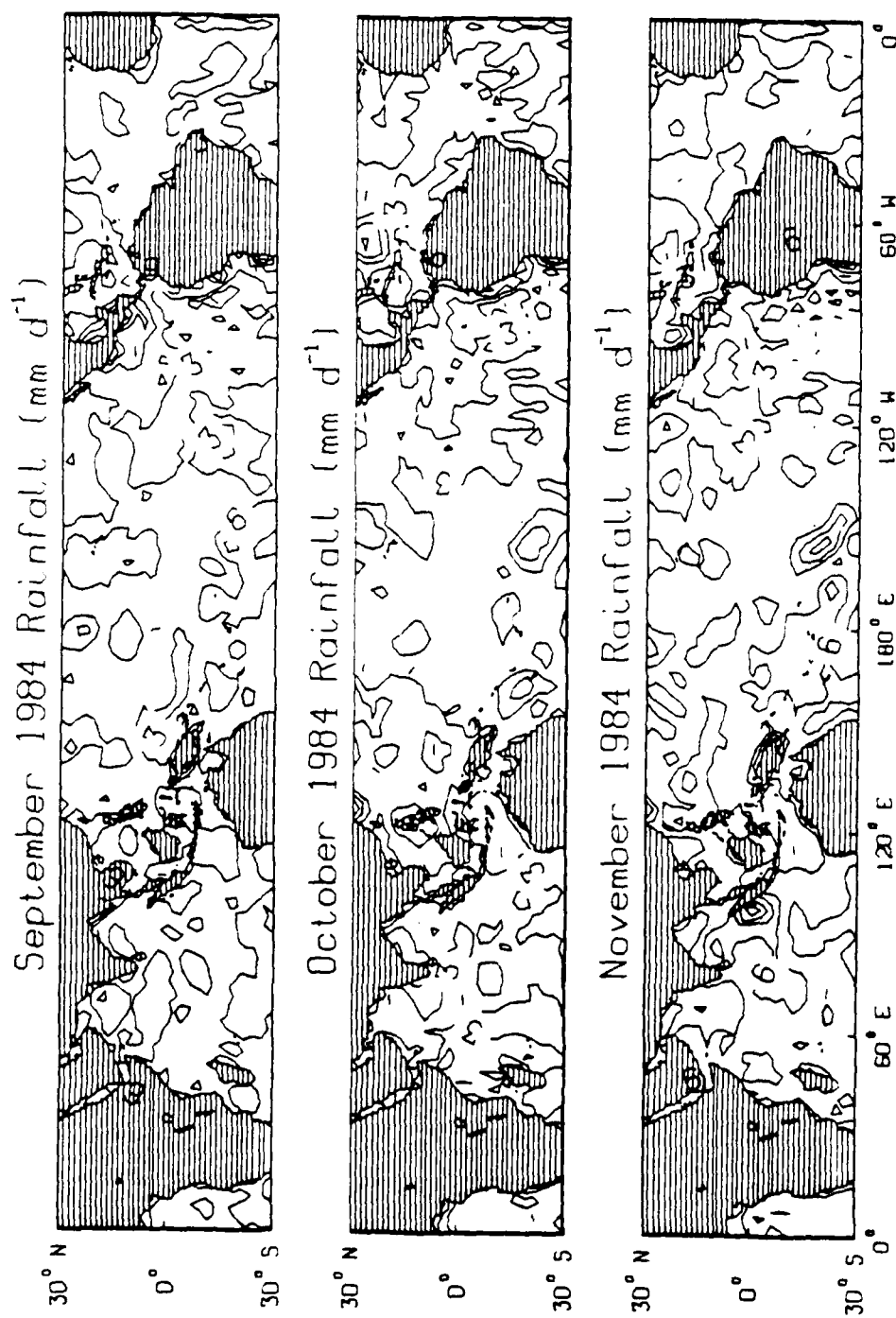
Figure A.2 Q_1 precipitation rate estimate for September, October, and November 1984.

59
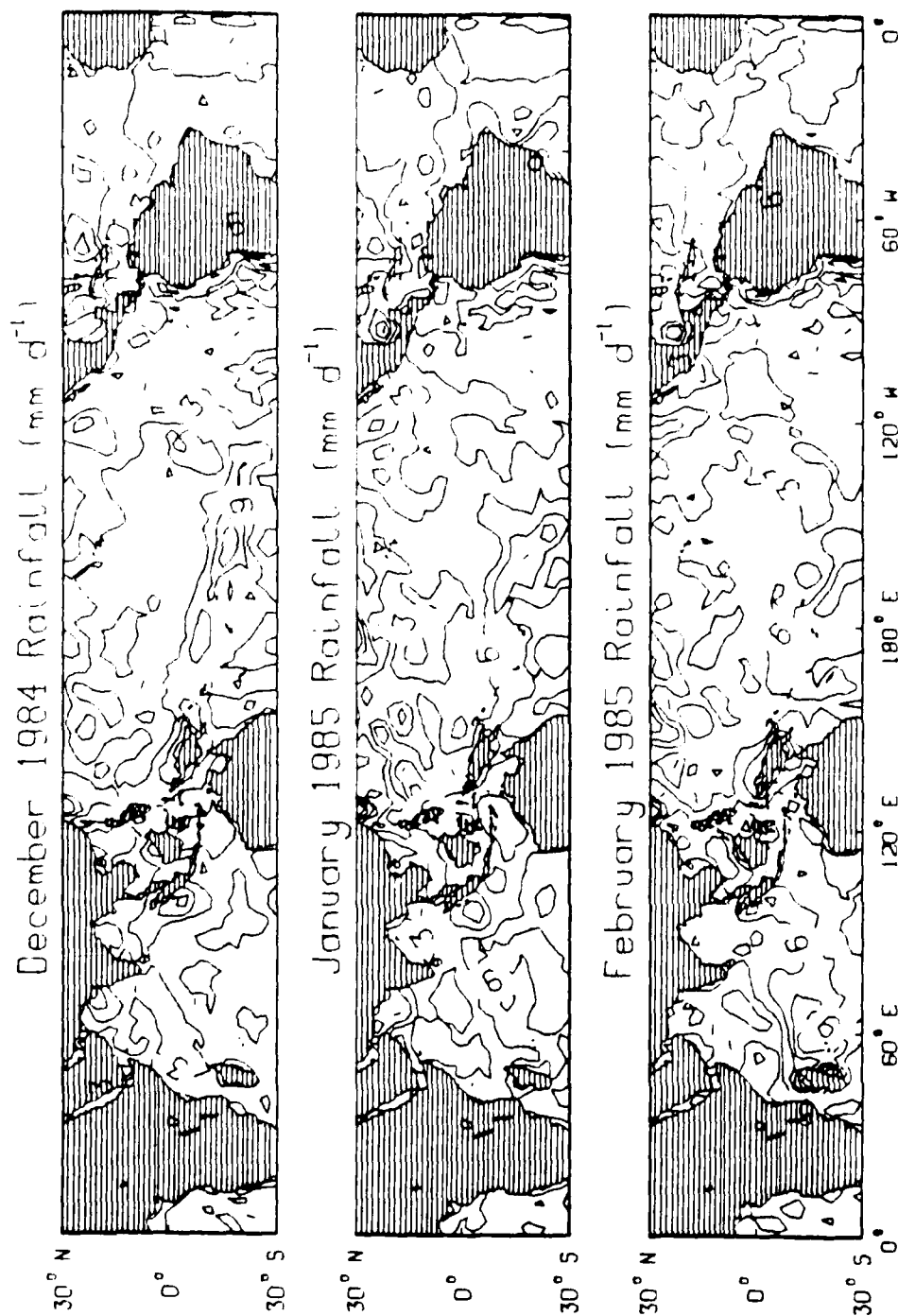
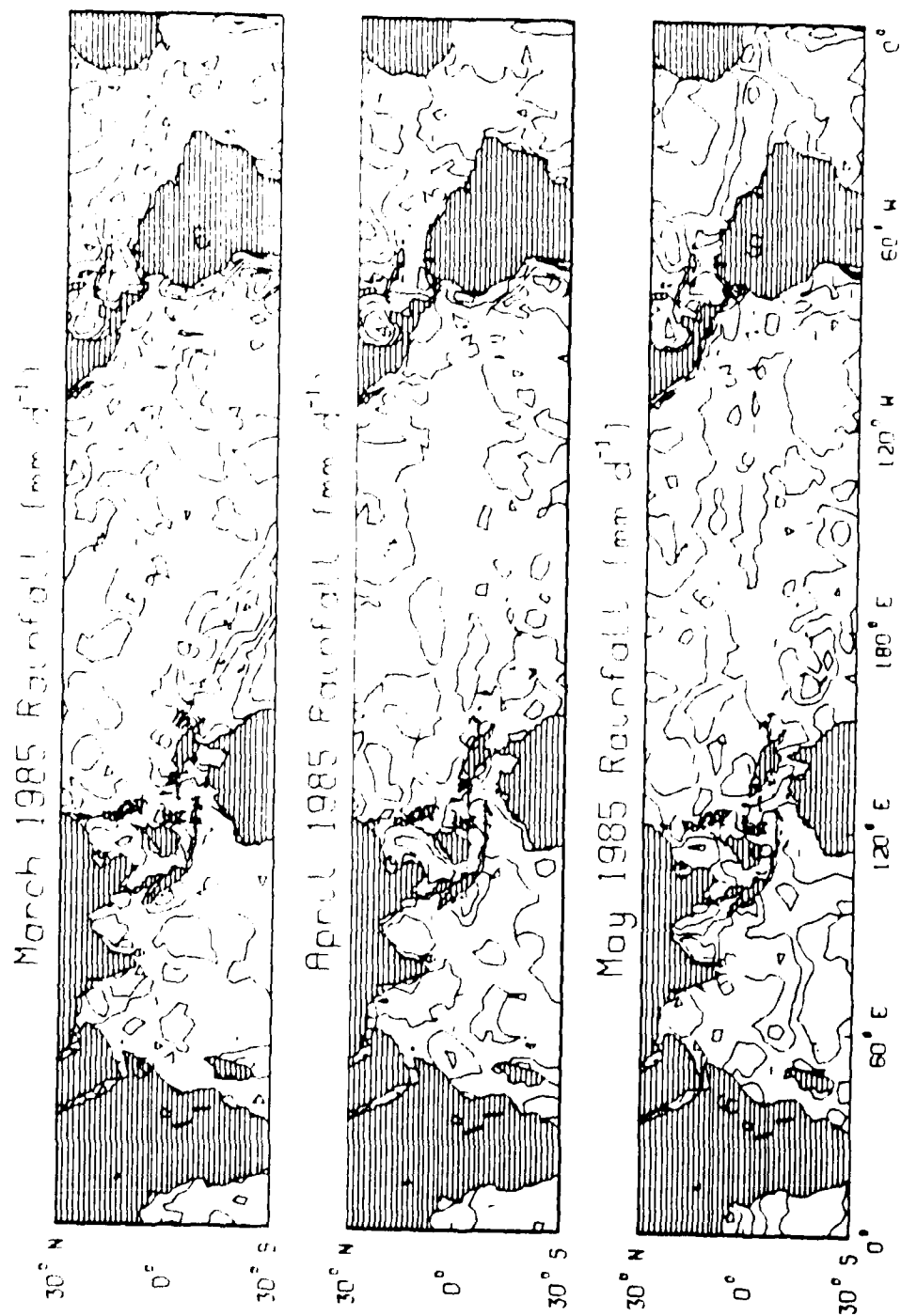Figure A.3 Q_1 precipitation rate estimate for December 1984, January and February 1985.

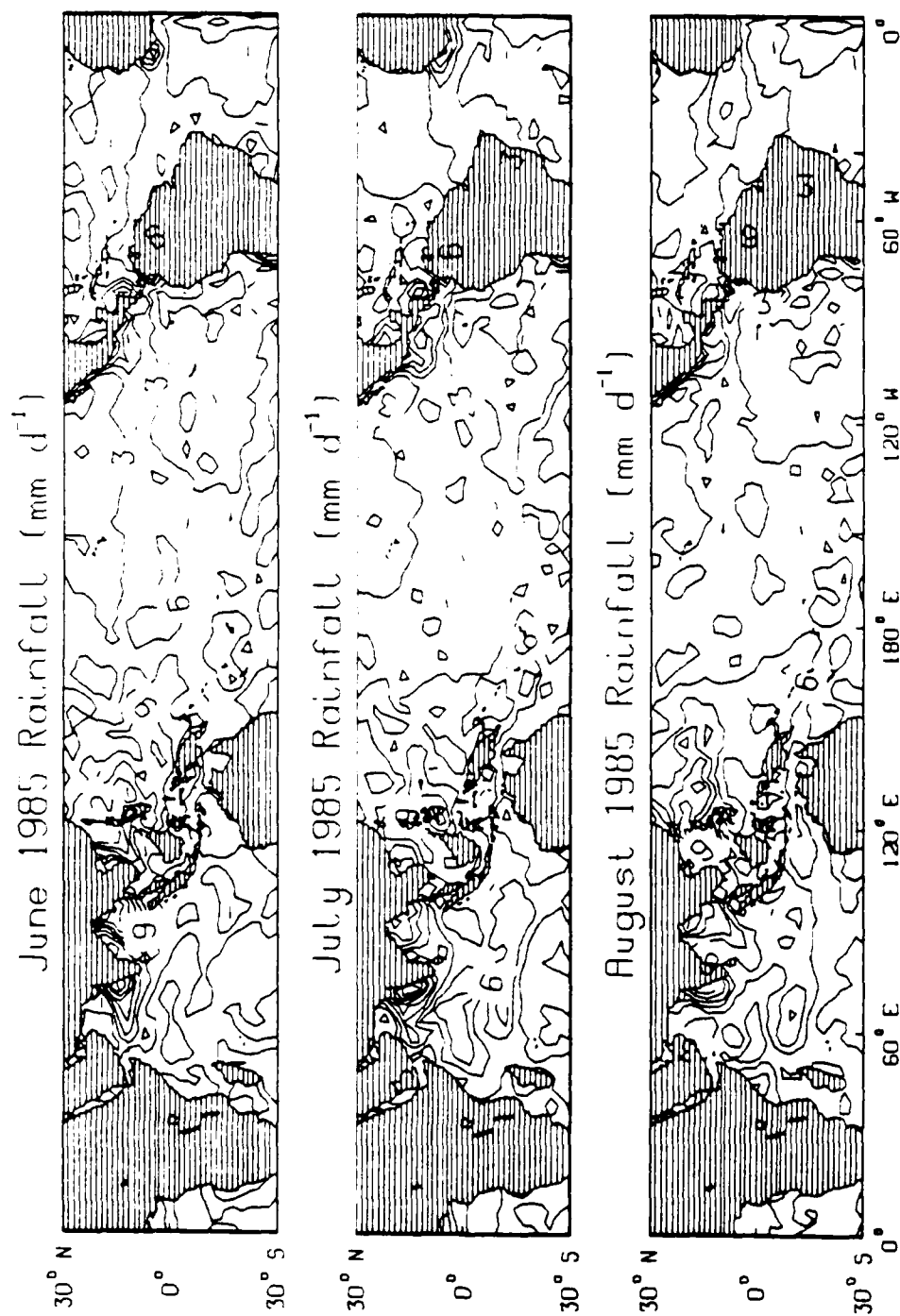Figure A.4 Q₁ precipitation rate estimate for March, April and May 1985.

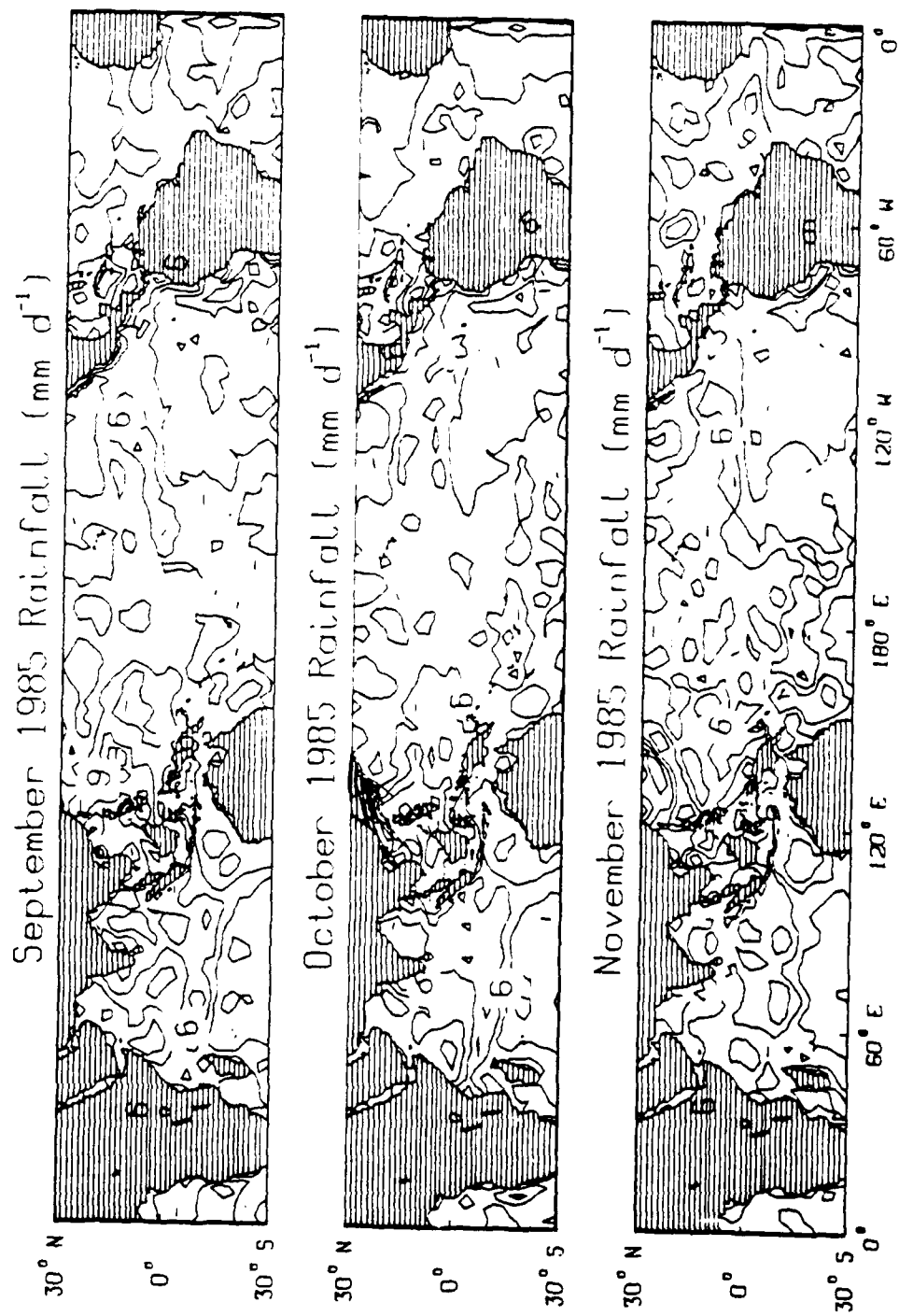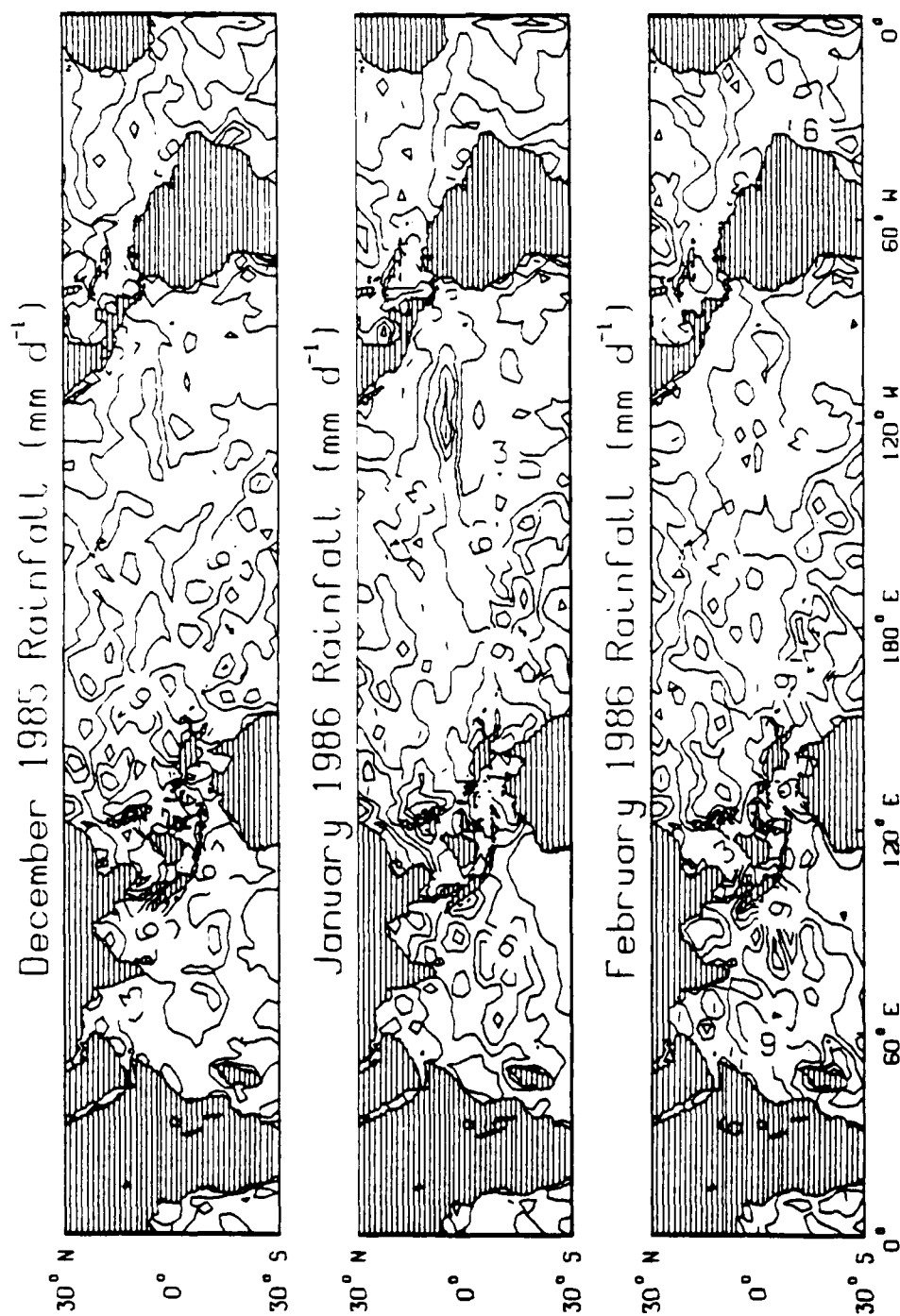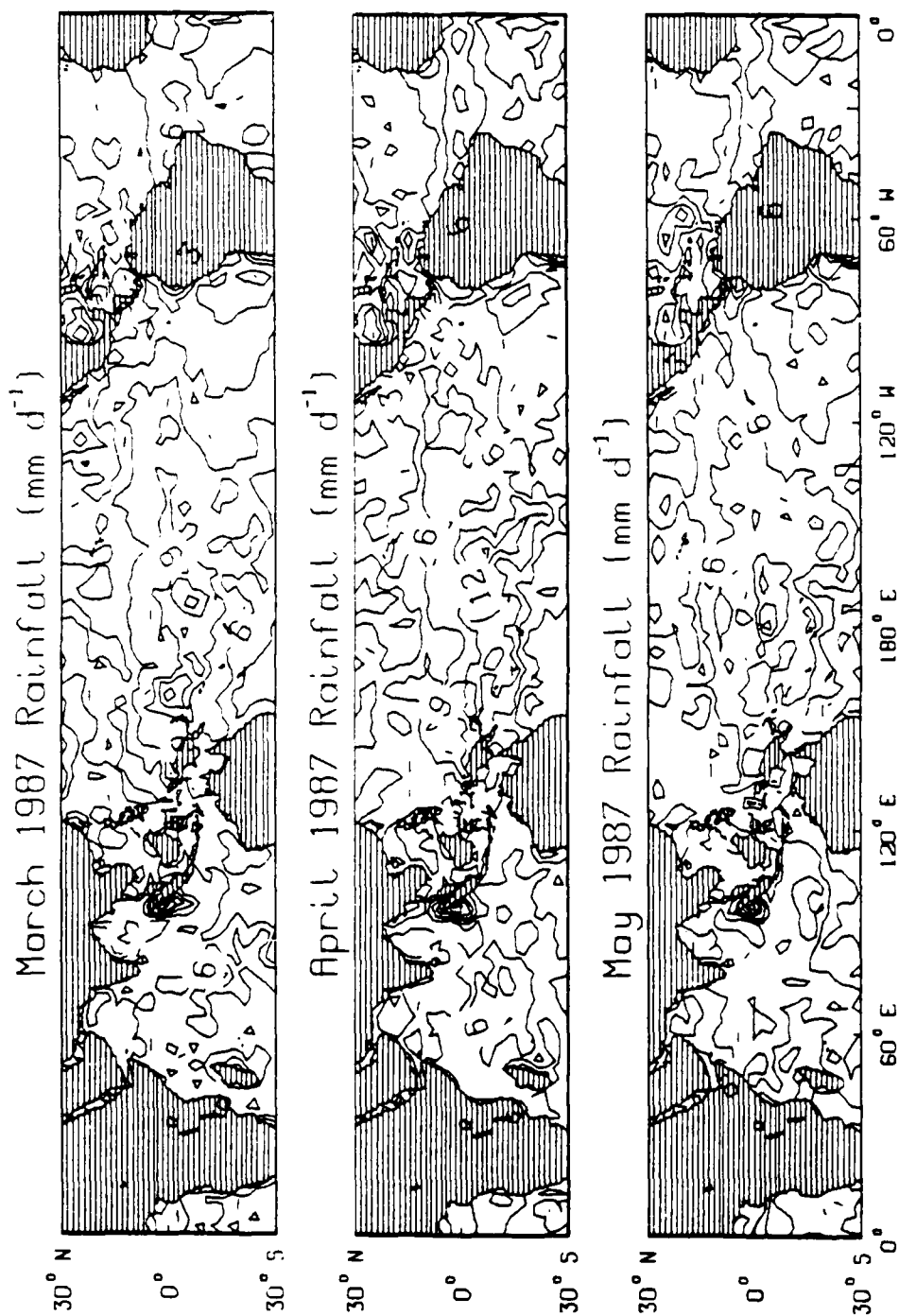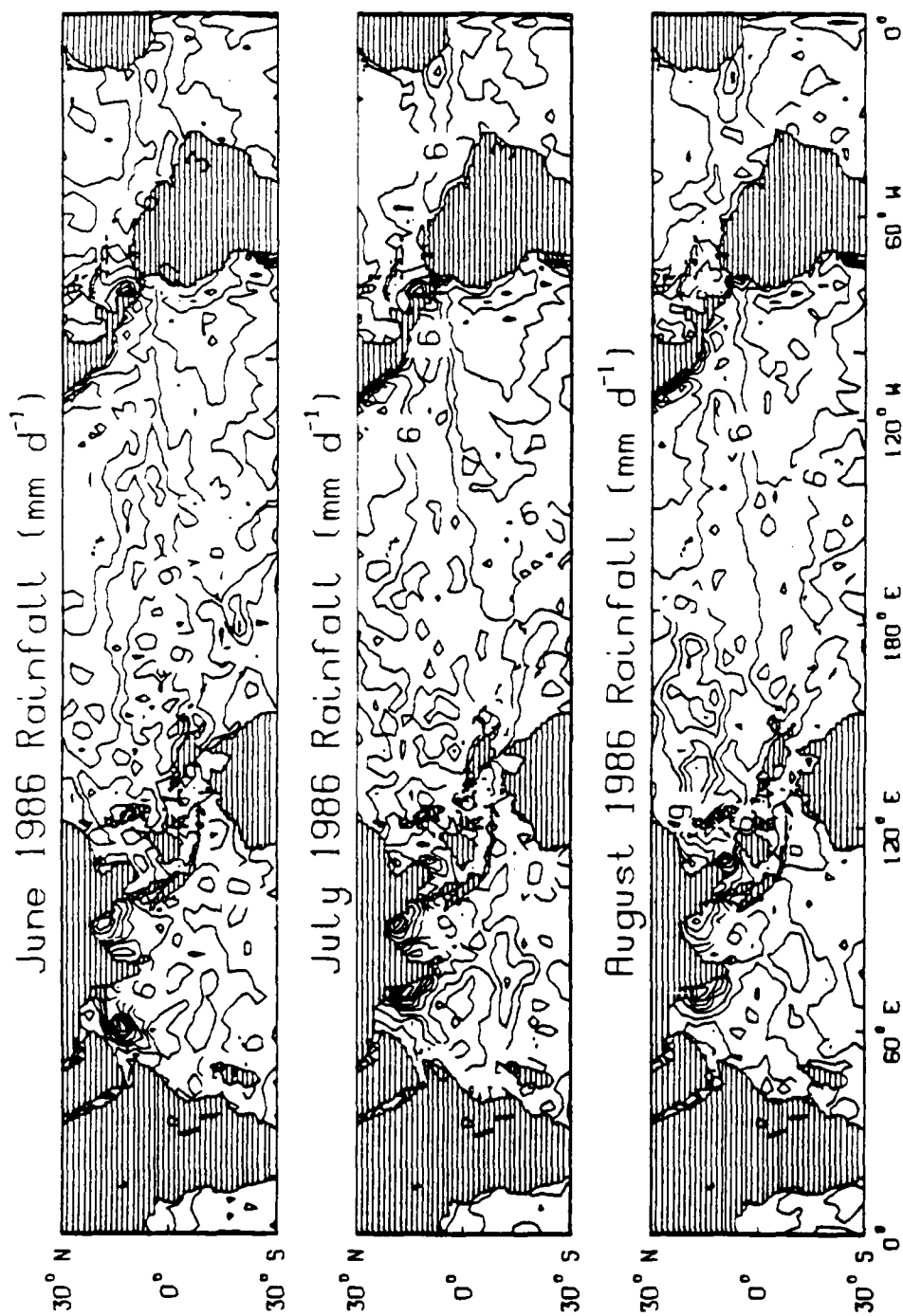Figure A.5 Q_1 precipitation rate estimate for June, July and August 1985.

September 1985 Rainfall (mm d^{-1})

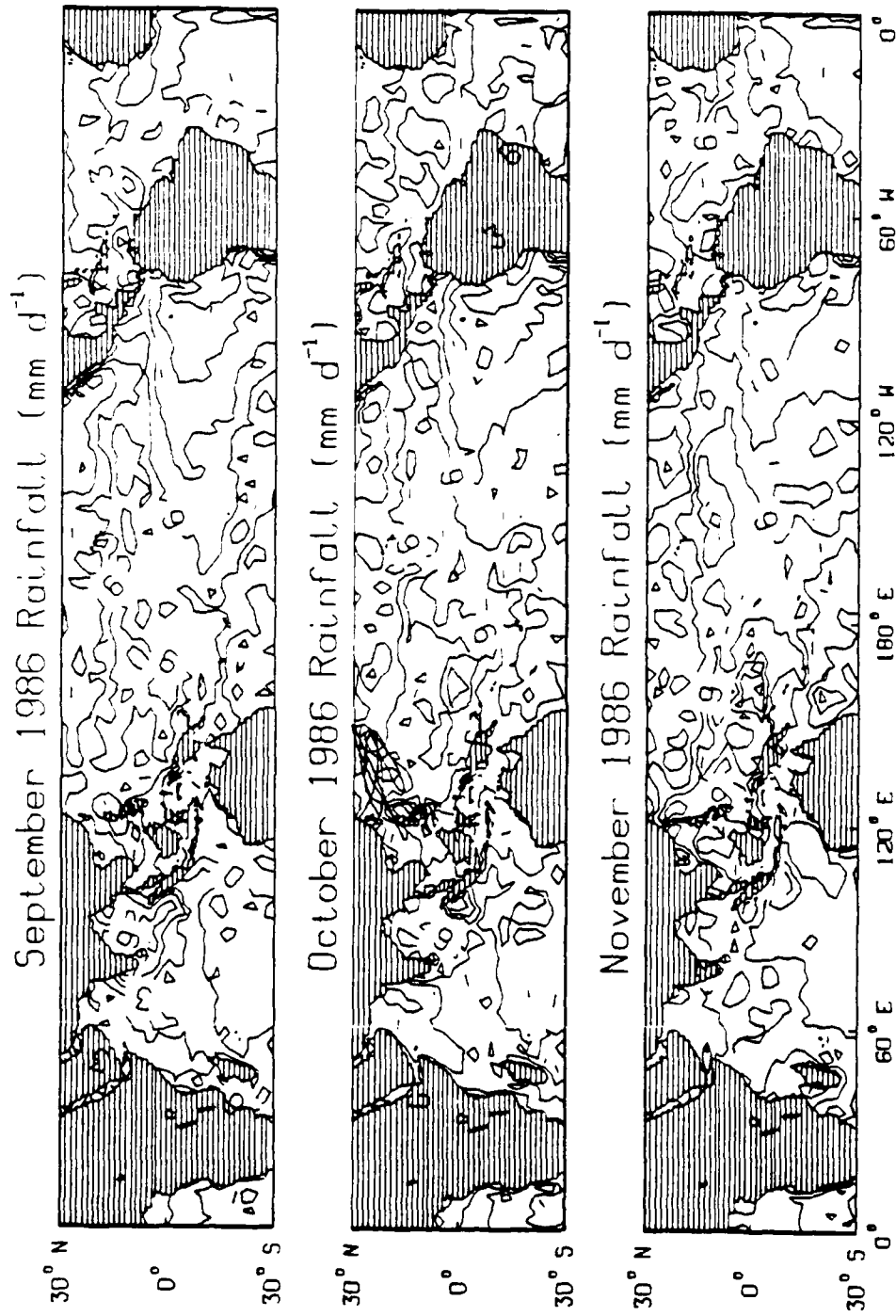October 1985 Rainfall (mm d^{-1})

November 1985 Rainfall (mm d^{-1})

Figure A.6 Q$_1$ precipitation rate estimate for September, October, and November 1985.

Figure A.7 Q1 precipitation rate estimate for December 1985, January and February 1986.

Figure A.8 Q_1 precipitation rate estimate for March, April and May 1986.

Figure A.9 Q_1 precipitation rate estimate for June, July and August 1986.

September 1986 Rainfall ($mm\ d^{-1}$)

October 1986 Rainfall ($mm\ d^{-1}$)

November 1986 Rainfall ($mm\ d^{-1}$)

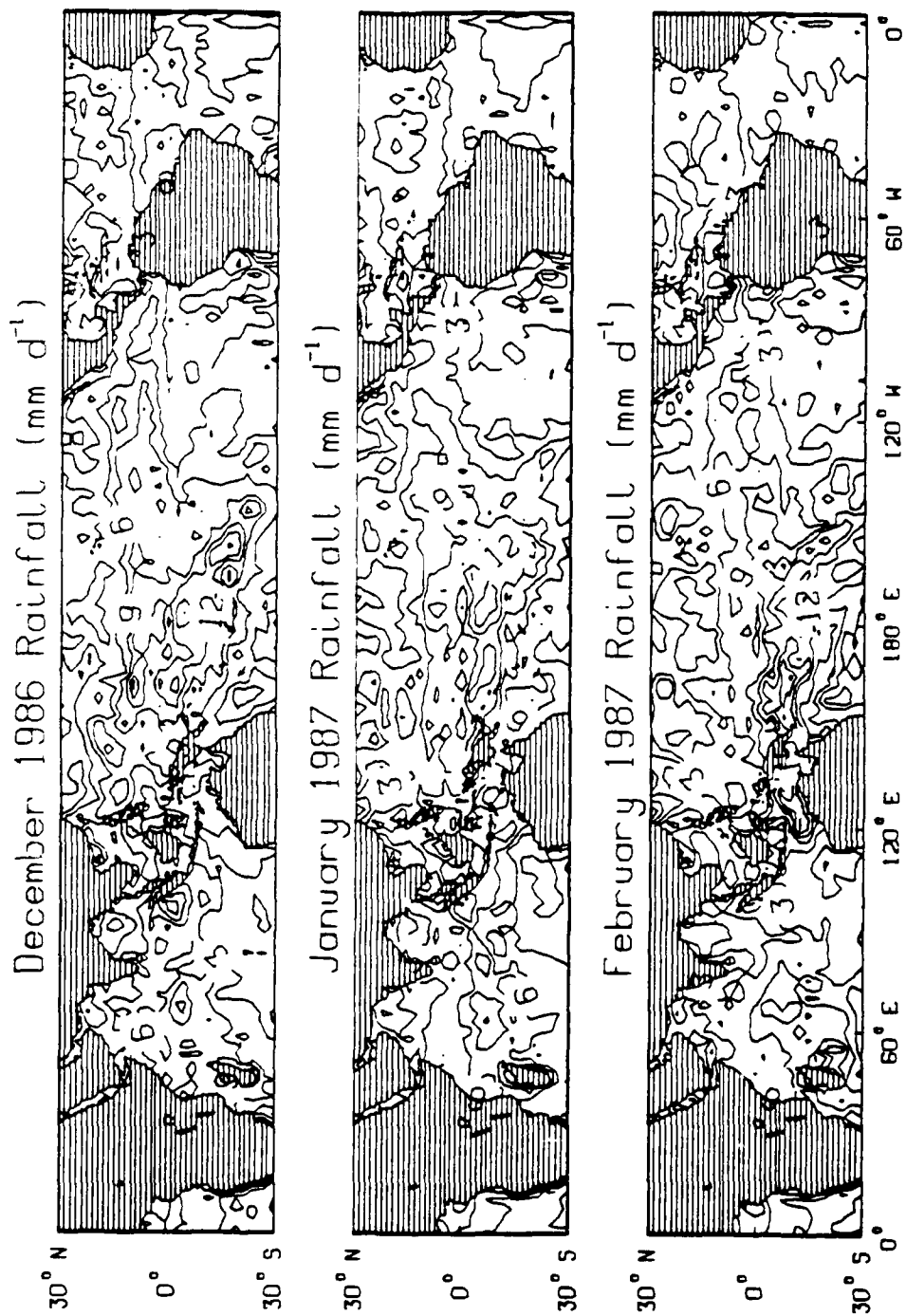Figure A.10 Q_1 precipitation rate estimate for September, October, and November 1986.

Figure A.11 Q_1 precipitation rate estimate for December 1986, January and February 1987.
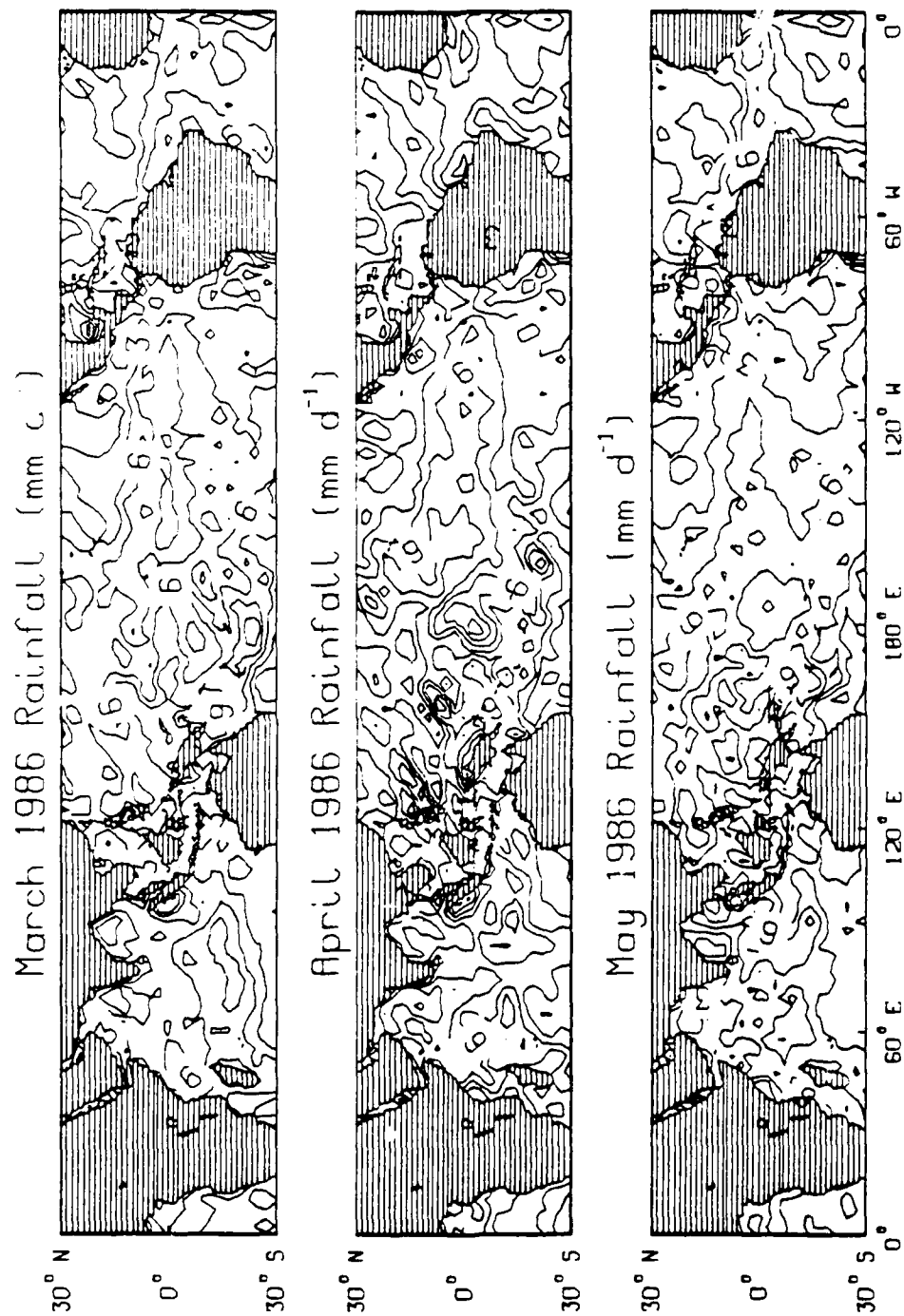
Figure A.12 Q_1 precipitation rate estimate for March, April and May 1987.